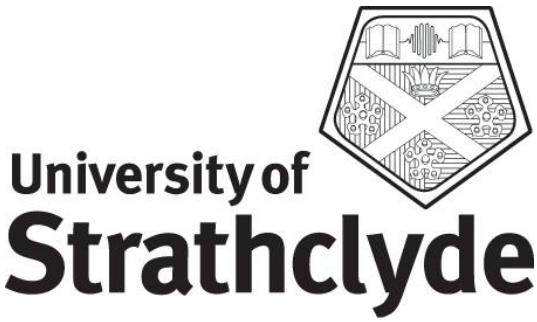

'Validation of an ultrasound-based navigation system for the assessment of femur anatomy'

Richard Allan

MSc Bioengineering

Bioengineering Unit

University of Strathclyde

Date of submission: 27/09/2011

‘This thesis is the result of the author’s original research. It has been composed by the author and has not been previously submitted for examination which has led to the award of a degree.’

Signed: **Date:16/08/2011**

Abstract

Purpose. Ultrasound-based navigation systems have been suggested as a viable alternative for surgeons to use to acquire the location of bone landmarks preoperatively, intraoperatively and postoperatively for orthopaedic procedures. The purpose of this project was to investigate the level of accuracy and precision of an ultrasound-based navigation system and to compare these results to the currently acceptable values.

Methods. An ultrasound system (TELEMED Echoblaster 128) and a navigation system (OrthoPilot, B. Braun Aesculap) were integrated to create an ultrasound-based navigation system. A validation test of the system was performed on a simple geometric object and then applied to a femur model comprising of 12 identifiable landmark locations.

Results. Initial validation of the ultrasound-based navigation system provided accuracy to within 0.5mm. Application of the system to the femur model resulted in a reduction in accuracy to ≥5mm for the majority of landmark locations. In terms of precision, the ultrasound-based navigation system produced repeated measure variability of ≤1mm (SD), ≤0.5mm (SE) for the majority of landmark locations.

Conclusion. The ultrasound-based navigation system provided results less accurate than the conventional methods used in orthopaedic procedures. Level of accuracy varied between axes with significantly reduced accuracy in the z-axis of the base plate coordinate system. The system provided a high level of repeatability for the majority of landmark locations. The results indicate that ultrasound-based systems could in time provide an alternative method of data acquisition to the current methods used during computer assisted orthopaedic surgery however further investigation is required.

Acknowledgments

I would like to take a moment to say many thanks to my primary project supervisor, Dr Angela Deakin for everything she has helped me with throughout the project. Furthermore I would like to say thank you to my second supervisor Dr Phil Riches who assisted me greatly in times of need. Finally I would also like to say a thank you to all the technical staff in the Wolfson Building, most notably Stephen Murray and John Maclean who managed to assist me with the technical aspects of the project. Without all these individuals I would not have been able to complete this project.

Table of Contents

1 Introduction

1.1 Background Information

Technological advances over the past 10-20 years have resulted in systems which use computers as an aid for navigation being introduced into the surgical environment. This increase in prevalence is evident within the field of orthopaedic surgery where these systems are extensively used during procedures such as total arthroplasty of the hip and knee. These systems benefit the operative procedure by accurately and instantaneously creating anatomical reference frames which can relate the position and orientation of an optical reference marker to the underlying bony anatomy. In essence they provide the surgeon with additional information allowing greater accuracy and precision during preoperative surgical planning, intraoperative navigation and postoperative check-ups.

Image free navigation systems have become one of the most common navigation techniques used in orthopaedic procedures. Pre-operative image systems which incorporate CT or MRI remains the best method however it is not viable for every procedure to be done to this standard. Image free data acquisition from direct contact with bony landmark acquisition has provided a suitable level of accuracy in orthopaedic procedures but is extremely invasive. Direct/percutaneous palpation has also been suggested as a method of addressing landmarks however this method is not viewed as sufficiently accurate. Focus within this area has moved onto newer methods of acquiring landmark locations. Ultrasound has been suggested as the solution to this problem by potentially providing an accurate, cost-effective, non-invasive method of acquiring bony landmarks. Although currently not viewed as a viable method of acquiring useful data due to the associated problems regarding image quality and the technical difficulties involved with the data there is great potential within the technology which could lead to newer, more accurate and more precise procedures introduced into computer assisted operative procedures.

1.2 Project Aims

This project aims at investigating the accuracy and precision of the ultrasound-based navigation system in 3 stages. Stage one focuses on the validation of the ultrasound-based navigation system by means of investigating its ability to locate basic geometric shapes. Stage two then expands on this by applying the system to the more complex object of a model femur bone. The final stage will then involve analysing which of landmark locations on the femur model the system is more accurate in detecting and discussing the reasons for this. The entire project is effectively investigating the accuracy and repeatability (precision) of this ultrasound-based navigation system and its possible benefits as a research tool and functional use.

2 Literature Review

2.1 Computer Navigation Systems

Computer navigation systems have been established as extremely beneficial tools during various surgical procedures (Delp et al, 1998; Mihalko et al, 2006). They are capable of providing highly accurate data in pre, intra and post-operative situations allowing a greater level of assessment to be made on the success/failure of the operation. How effective the system is depends on the accuracy and precision of the navigation as well as the capability of the user. Di Gioia (1998) reported several steps required for an effective computer navigation system; a full preoperative plan, successful intraoperative registration relating the preoperative images with the patient's anatomy and position on the operating table and the accurate tracking of the position and movement of bony structures and tools throughout the procedure.

Computer navigation systems, sometimes referred to as passive systems, generally fall under two main categories; Image-based and Image-free. Image-based navigation systems rely on data acquired from pre or intra-operative imaging techniques. Most commonly these involve computed tomography (CT) or magnetic resonance imaging (MRI). However intra-operatively these methods cannot be used as the process of acquiring MRI/CT data during a surgical procedure is extremely difficult which requires a highly specialized facility. Intra-operative imaging techniques have most commonly involved fluoroscopic techniques (Van Damme, 2005) in their data acquisition. Image free navigation systems on the other hand rely on the acquisition of specific anatomical points to recreate a model of the specific structure of interest. Previously this has been achieved using direct or percutaneous probes (Di Gioia, 1998)

2.2 Principles of Image-free Navigation Systems

Conventional data registration methods have involved invasive procedures which rely on the position sensing probe to be in direct contact with the bone surface. This registration process is normally achieved by removing the soft tissue during surgery to expose the bone and the points registered using a mechanical pointer (Brin et al, 2010).

One of the most important aspects of any image free systems is the data acquisition stage. Simon (1996) stated that the success of registration depends on numerous factors including; the number of points collected, the distribution of the points and the number of areas with unique geometric configurations on the object surface.

In terms of TKA, image-free navigation systems require the intra-operative registration of specific anatomical landmarks. These landmarks are then used to determine the mechanical alignment of the tibia, femur and the lower limb (Pitto et al, 2006). These consists of the most proximal and distal points; the centre of the femoral head and the centre of the ankle joint. Furthermore points are also registered around the knee. The determination of these locations allows the determination of the tibial and femoral mechanical axis allowing the position of the cuts to the bone for the implantation procedure to be calculated (Pitto et al, 2006).

2.3 Ultrasound

Ultrasound functions on the basis of the speed of sound. When pulses of sound waves travel through air and contact a solid object they are reflected. From knowing the speed of sound calculations can be made to determine the distance between the object and scanner. As the name suggests ultrasound operates at a frequency above the range of normal human hearing, above 20 kHz. The majority of medical ultrasound devices function at frequencies between 1 - 10 MHz (Lockwood et al, 1996). Technological advances in ultrasound have resulted in the operating frequencies increasing substantially to over 100 MHz for procedures such as ultrasonic microscanning of the eye (Vogt et al, 2010). However there is a trade-off between the level of penetration and the resolution of the image based on the frequency at which the ultrasound operates at. The attenuation of ultrasound increases approximately linearly with frequency in soft tissues limiting the penetration depth. Common procedures such as scanning the abdomen typically use frequencies between 3-5 MHz to provide the best compromise between resolution and tissue penetration. (Wells, 1999).

The generation of ultrasound is obtained using piezoelectric effect that is when materials with piezoelectric properties are subjected to pressure, an electric charge appears across the surface of the material. Ultrasound is generated using the converse of this concept whereby a voltage is applied to the piezoelectric material resulting in a change to the thickness of the material. Depending on the nature of the wave required short, long or continuous electrical pulses are applied to a piezoelectric transducer. This causes the material to vibrate at a specific frequency which is dependent on the thickness of the piezoelectric material. The detection of ultrasound occurs in a similar way but reversed. The vibrations contact the piezoelectric material causing it to vibrate creating small electric charges on its surface. These electrical charges returning to the transducer are then processed electronically to allow the information to be presented in a useable way i.e. monitor display (McDicken, 1981).

The piezoelectric material used will also affect the characteristics of the ultrasound wave. Current medical ultrasound devices commonly use piezoceramic materials such as PZT (lead zirconate titanate) or lithium niobate. These materials are beneficial as they have a faster response, are far more stable and have a greater level of sensitivity compared to other piezoelectric materials (Xu et al, 2006).

Ultrasound can function in various modes which describe how the ultrasound is applied to the object. By far the greatest application of the imaging technique used in medicine today is in the field of obstetrics. In this area clinicians use the ultrasound technology to obtain information about the foetus with regards to its health and progression. Various modes can be used in order to find the optimal outcome. Surgical navigation systems however require a complete structure to be registered and this is done using two main methods; A-mode (Amstutz et al, 2003; Heger et al, 2005) and B-mode (Amin et al, 2001; Kowal et al, 2001). A-mode or amplitude mode represents the time required for the ultrasound beam to strike a tissue interface and return its signal to the transducer. Therefore the greater the reflection at a tissue interface, the larger the signal amplitude on the A-mode screen. In B-mode or brightness mode the bright dots which appear on a screen represent the echoes returning to the transducer. On the 2D image the vertical position of each bright dot is determined by the time delay from the initial transmission of a pulse to the return of the echo, and the horizontal position is determined by the location of the receiving transducer element. In B-mode these returning echoes appear with different shades of darkness depending on the intensity of the returning sound waves (McDicken, 1981).

2.3.1 Advantages of Ultrasound

Along with CT and MRI, ultrasound is used widely as a diagnostic tool in medicine. Presently ultrasound is estimated to account for approximately 20-25% of all imaging procedures worldwide and growing. It has numerous advantages as a preoperative and intraoperative imaging technique. One of these advantages is that it

is non-invasive. Ultrasound does not require any anaesthesia or pain relief during its operation. Furthermore the ultrasound scanner acquires the data transcutaneously requiring no damage to the soft tissue.

Ultrasound is a non-ionising form of imaging making it safe for the patient. In the United States alone over 62 million preoperative CT scans are performed every year (CT market study, 2006), all of which add to the total radiation. Although there are other known intra-operative imaging techniques of better image quality such as fluoroscopy (Zheng et al, 2006) they also expose the patient to radiation. Ultrasound has the advantage both pre-operatively and intraoperatively to these methods of having no radiation exposure for the patient.

One of the leading factors in the development of new non-invasive imaging techniques involves the potential reduction in the financial costs to public and private health services. A review article published by Fletcher et al (1999) reported that the cost of running an MRI facility per year in 1996 was approximately £434,000 at a cost of roughly £115 per scan. Taking into account the cost of the MRI scanner on top of that the NHS spends close to £2 million pounds within the first year of every MRI installed (nhs.uk). Therefore the development of new non-invasive techniques which provide the same level of accuracy as MRI but at the fraction of the cost could effectively save health services hundreds of thousands if not millions of pounds.

2.3.2 Disadvantages of Ultrasound

The use of sonography as a method of determining spatial measurements does have numerous difficulties associated with it in terms the efficacy of its use. Currently, non-invasive ultrasonic bone imaging techniques are not viewed as an adequate method in clinical practice due to its limitations in terms of image quality, accuracy and precision (Krysztoforski et al, 2011). Variations exist between the acoustic properties of the soft tissues of the human body. As a result of these differences the speed of sound will vary between the soft tissues resulting in the potential for error. Christensen et al (1978) reported that the speed of sound in soft

tissue ranged from approximately 1450 m/s in fat to 1600 m/s in muscle. Diagnostic ultrasound evaluations for many years have been performed based on the average value of the speed of sound in the various tissues, which has been found to be approximately 1540 m/s (Goss et al, 1978). As a result of this assumption there could be significant errors introduced with regards to the correct location of the bone surface.

As stated previously these variations which exist between the acoustic properties of materials/tissues can lead to potential errors. Non-medical testing involving ultrasound is normally carried out in a water bath to give an acoustic "contact" to the object. In this setting the acoustic properties of sound waves will result in the speed of sound in water at room temperature being slower than its speed in average soft tissue. Studies have indicated that this variation in speed of sound can give rise to systemic errors of approaching 5% (Barratt et al, 2006; Balaniuk and Wong, 1993). It has been suggested that for a linear ultrasound probe this systemic error can be removed by applying a correction factor to the results. Bilaniuk and Wong (1993) stated that this correction involved the translation of each likely edge point toward the probe face. Therefore the axial coordinates *y* of the points is multiplied by a temperature correction factor of;

Barratt et al (2006) investigated a new approach to the speed of sound problem by developing a 'self-calibrating' ultrasound system. The standard calibration method for ultrasound systems involved scanning a phantom area containing objects of known geometric dimensions. The differences in speed of sound between the calibration stage and the *in vivo* stage were taken into account by updating the calibration parameter values taken throughout the procedure using a preoperative phantom calibration whilst at the same time using ultrasound to register surface points on the bone. This method avoids the acoustic problems by using the bone as an *in vivo* calibration object resulting in the calibration parameters being continuously updated based on the *in vivo* data.

Another disadvantage with ultrasound technology is the image quality as well as the technical challenge associated with processing those images. The low imaging quality, especially in bone, is due to the reflection of the ultrasound waves at the interface between the soft tissue and bone. Both CT and MRI provide superior image quality compared to ultrasound due to their ability to differentiate between the various tissues present within the body. CT scans are commonly taken preoperatively for procedures involving bone as the x-rays provide the highest quality of imaging allowing easier interpretation.

2.4 Accuracy and Precision of Computer Navigation Systems

With all measuring devices it is important to note that the terms accuracy and precision have to be defined separately. The accuracy of a system is defined as the maximum amount by which a result differs from the true value. The precision of the system is defined as the level of agreement between repeated measurements (Beckwith et al. 1982). It is important to distinguish between these two characteristics as a computer navigation system can have both, either or none, all of which affects it's suitability for the task.

The accuracy of tracking systems used in computer navigation involves the optimal interaction between both the hardware components, including the tracking camera and the reference frames and the software components of the system. Studies have indicated that the accuracy of these systems can range from approximately 0.5–3mm (Khadem et al. 2000). Furthermore a study by Li et al (1999) investigated the angular accuracy of such systems and found its accuracy to be approximately within 1°.

The accuracy and precision at which computer navigation systems operates have a massive impact on their efficacy. Siston et al (2007) reported that the inaccurate location of landmarks can lead to significant errors in the orientation within the coordinate system. Small inaccuracies in the landmarking stage could create a 'snowball effect' leading to an accumulation of much greater inaccuracies.

Standard point-based registration methods commonly used during Computer Assisted Orthopaedic Surgery (CAOS) of the hip and knee have been extensively researched in terms of their accuracy and precision. CAOS itself is the discipline where computer technology is applied pre-, intra- and/or post-operatively to improve the outcome of orthopaedic surgical procedures. Studies within the literature have reported errors ranging between 0.5 to 5 mm using this method (Lavallee et al, 1996; Sugano et al, 2002; Hufner et al, 2003). Several studies have also reported computer

assisted surgery precision values to be ~1mm (Hufner et al, 2006; Picard et al, 2007). The results of these studies reinforce the idea that direct contact to landmark locations provides the most accurate results. Furthermore Sadowsky et al (2002) compared standard point-based, invasive registration methods to image-based, non-invasive registration methods. Their results showed a mean deviation of 2.75 mm for the image-based, non-invasive registration and a mean deviation of 0.5mmfor the contact-based, invasive registration.

Clinically, one of the most widely studied areas regarding the accuracy and precision of computer navigation systems has involved limb alignment. Studies have focused on using phantoms as well as comparing data from navigation systems to pre-operative imaging such as 2D CT data to determine the level of accuracy and precision of the limb axis alignment (Keppler et al, 2004).

The accuracy of limb axis alignment has a major impact on the longevity of an implant. Studies have extensively investigated the effect of inaccurate limb alignment and the possible reasons for this (Brin et al, 2010). One of these proposed reasons of axis inaccuracy in navigated TKA is in the incorrect digitisation of anatomical landmarks. TKA incidence is much greater in elderly patients who have underlying health conditions such as osteoarthritis resulting in abnormal leg alignment. Such conditions will alter the knee anatomy of the patient and increase the difficulty of anatomical landmark recognition. There have been few studies which have investigated abnormal leg alignment. One study by Pitto et al (2006) demonstrated high accuracy of an image-free navigation system *in vitro* in both normal and abnormal leg alignment settings.

Within the literature navigation systems are used extensively in procedures focused around the hip and knee. Procedures such as TKA and THA rely heavily on the navigation systems providing accurate and precise locations of the specific anatomical landmarks which are crucial during surgery. It is this accuracy and precision of the system which determines the operations success or failure.

Currently very little data exists that describe how accurately landmarks must be presented to the system. These data are crucial in the case of image-free

navigation because the system's frame of reference is based solely on the information provided by the surgeon during the acquisition stages

2.5 Navigation during knee surgery

One of the areas which has benefited significantly from the technological advances in computer systems is orthopaedics. As a result of this there has been a dramatic rise in the use of computers as a form of aid during orthopaedic procedures. Over the past 5-15years CAOS has been applied to a wide range of orthopaedic procedures ranging from basic fracture surgery (Hufner et al, 2003) to tibial osteotomies and total replacement of both the hip and knee (Amiot and Poulin, 2004).

Many subsets exist within CAOS dealing with various aspects of its use. One such subset which has received significant attention in recent years has been the development of more accurate navigation and surface registration methods used in surgical procedures. These systems provide the surgeon with the technology to allow a greater accuracy of preoperative surgical planning, intraoperative navigation and postoperative review (Barratt et al, 2006).

These navigation systems were introduced in order to provide a higher level of precision of implantation compared to conventional instruments. They use bony landmarks to collect accurate, instantaneous information regarding joint position and motion during surgery. The benefits of such systems can be seen during TKA as the navigation system provides the surgeon with an easy to follow guide for optimal alignment of the prosthesis (Matziolis et al, 2007).

Image free navigation techniques used in knee procedures such as TKA involve the acquisition of data which enables the surgeon to build a reference frame of the knee. In the majority of procedures temporary trackers are attached to the bone at strategic locations around the joint and viewed with an infrared system. This provides real-time spatial anatomical data regarding position and orientation of the leg (Brin et al, 2010). The surgeon then selects specific anatomical landmarks by using a digitiser attached to an infrared tracker. The navigation system uses the landmarking of the anatomy to create reference frames of the tibia and femur locations. From this the surgeon can determine where on the bone the cuts should be

made as the system provides real-time positioning of the cutting blocks relative to the bony anatomy.

One of the most well established benefits of using computer assisted navigation is in re-establishing the alignment of the lower extremity to the mechanical axis, one of the fundamental goals in procedures such as total knee arthroplasty (Sparmann et al, 2003) and high tibial osteotomies (Sprenger et al, 2003). Studies have shown that TKA procedures which employ a computer navigated approach have shown a significant improvement in accuracy and reduction in error in the implant alignment and placement. Mihalko et al (2006) compared the difference in tibial axis alignment between traditional intramedullary and extramedullary alignment techniques and computer navigated alignment. They concluded that the direct measurement of the mechanical axis using computer navigation for the tibia resulted in a higher level of accuracy compared to standard techniques.

The postoperative mechanical axis alignment of the limb achieved using navigation systems has also been extensively investigated. Clinical studies have indicated that navigation systems provided significantly better restoration of the neutral alignment of the mechanical axis of the lower limb compared to standard alignment methods (Bathis et al, 2004; Haaker, 2005)

Furthermore another important factor in total knee replacements involves maintaining the correct rotational alignment of the prosthesis. This has been achieved from using Whiteside's Line intraoperatively to assess the rotational femoral alignment (Middleton & Palmer, 2007). Whiteside's line uses the positioning of the intercondylar notch and femoral trochlear to create an imaginary line to which rotations can be assessed from Therefore in order to assess the rotational alignment of the prosthesis these locations must be must be accurately located.

Studies which have investigated the outcome of TKA have also reported that the success of an operation is greatly influenced by the surgeon's ability to accurately identify and register the anatomic landmarks (Delp et al 1998). Inaccurate registration of the anatomic landmarks can lead to potential errors in the procedure.

If there are errors within the position, orientation and/or alignment then this can lead to wear of the implant leading to failure. Ritter et al (1994) reported that tibial bone cuts that were varus by > 3° where associated with increased likelihood of implant failure and loss of function. Furthermore Mason et al (2007) demonstrated that CAOS provided a 30% improvement in the positioning of total knee prosthesis in the frontal plane compared to a standard technique when the optimal position was assumed at ± 3°.

Point based registration to 3D CT images is still regarded as the gold standard method used during computer assisted surgery (Murtha et al, 2008). However one of the major disadvantages of procedures which require point based registration is that they are highly invasive. Complications such as damage to the soft tissue, increased blood loss, and increase chance of infection are potentially increased as a result of these procedures. The development of new non-invasive imaging techniques will promote less invasive procedures resulting in a greater degree of safety and lower risk of complication.

2.6 Ultrasound and Navigation

For the past decade ultrasound has been proposed as a non-invasive alternative for localizing bone surfaces (Lavalée et al, 1996). The ultrasound and navigation system combine by tracking an infrared emitting body mounted on the ultrasound probe within a fixed space. Infrared cameras track the position and orientation of the transducer probe with respect to an externally fixed coordinate system. This setup effectively turns the US probe into a digitizer, similar to point based navigation systems. The surface points derived from the ultrasound are then used as the input data to generate a surface based model.

As stated previously the main advantage that ultrasound imaging has as a registration tool is that it is non-invasive, allowing a far larger area of the bone to be sampled compared to conventional methods. Standard point-based methods normally used during surgery are not suitable for minimally invasive procedures where there is limited access to the bone. Ultrasound imaging manages to avoid this problem by allowing registration of the bone surface through the soft tissue (Lavallée et al. 2004)

There have been few studies which have incorporated ultrasound and navigation most of which have been exploratory studies involving phantoms. These studies focused on using the intra-operative approach of navigation through ultrasound without requiring a preoperative CT scan. One such study by Lavalée et al (2004) tested the application of ultrasound and navigation on plastic bones and simulated soft tissue. There results showed a maximum surface error of 1.5 mm. Furthermore Chan et al. (2004) investigated the use of ultrasound for registration of bony anatomy in cadavers. Using ultrasound they registered statistical shape models of three femurs and two pelvises to surgical space. They then compared the results of the generated statistical shape model to a pre-operative CT image. The results of the study showed that the RMS of the ultrasound model was in the range 1.83–3.72 mm of specific anatomical regions of the femoral head and acetabulum.

In a similar study Murtha et al (2008) investigated the accuracy of ultrasound based registration to MRI and compared it with standard point based registration

methods. They found that the average RMS distance of the ultrasound based registration to MRI was 0.76 mm. This value was similar to the average CT RMS distance of 0.59 mm. From these results they concluded that the accuracy of ultrasound registration to MR surface models was accurate enough in terms of meeting the requirements of computer assisted surgery.

Research into the application of ultrasonography in the clinical setting has been sparse. One area which has seen some research involves the determination of the femoral head. In TKA the determination of the centre of the femoral head is critical in order to obtain the accurate alignment of the mechanical axis of the femur, essential for correct implant alignment. Matsuda et al (2003) investigated the reliability and reproducibility of identifying the centre of the femoral head using ultrasonography. In the study they identified the centre of the femoral head to within 5mm in 56% of patients and within 10mm in 81.6% of patients even within an obese group using ultrasonography. From the results they concluded that ultrasonography produced highly reliable results correctly aligning the mechanical axis to within 2° of the perfect alignment, a result which is extremely close to the clinically acceptable value of 1° stated by Li et al (1999). These findings were comparable to results obtained from conventional X-ray. In addition, Barratt et al (2006) reported that one of the main advantages of ultrasound-based registration, particularly when B-mode imaging was employed, was that the number of surface points that could be acquired was far greater compared to manual digitization by direct contact. They concluded that the registration accuracy could potentially be increased and the sample time reduced using ultrasound-based registration methods.

3 Methodology

To investigate the use of navigation and ultrasound in the identification of femur anatomical bony landmarks the following methodology was developed.

3.1 Equipment & Materials

A number of difference pieces of equipment were used in this study. These include the various parts of the Ultrasound and Navigation Systems as well as the formation of the Base Plate. These will be described in greater detail in the following subsections.

3.1.1 Ultrasound System

The ultrasound system consisted of both hardware and software. These will be detailed in the following subsections.

3.1.1.1 Hardware

The ultrasound system hardware comprised of an EchoBlaster 128 2D beamformer with a 6 MHz electronic linear probe (TELEMED Echoblaster 128; Telemed, Vilnius, Lithuania). The beamformer was connected to the user PC via USB (Fig 3.1)

Figure3.1 Layout of the Ultrasound System Hardware including probe and beamformer

3.1.1.2 Software

The software components used in the ultrasound system comprised of the Echoblaster® user interface (Fig 3.2). Within the EchoBlaster ® interface a wide variety of settings were altered to obtain the optimal image. A B-mode imaging mode was selected as the imaging method for the project with a dynamic focusing mode. This mode provided eight active focal zones and eight positions of transmit focus which could be manually selected. This provided a higher imaging quality as the sampling frame rate was at the optimal level, i.e. the images displayed per second provided the best possible picture. The parameters available for alteration can be seen in Fig 3.2. There were four distinct areas of control; Focus Control, Power Control, Gain Control and TGC Control. The Focus Control section included the settings of interest such as the transmit focus depth, the scanning depth, dynamic range and image enhancement. The dynamic range affected the image contrast

removing the grainy effect. The image enhancement setting allowed the image to be smoothed or sharpened giving better object perspective, i.e. the position of the object in the ultrasound image is a true reflection of its actual position. The power control slider controlled the percentage of acoustic power output from the beamformer. The Gain Control slider altered the voltage amplitude of the signal resulting in changes to the brightness of the image. The TGC control had five sliders allowing the gain to be adjusted for specific depths. On the right hand side there was also the Palette Control and Rejection Filter. The Palette Control sliders allowed the brightness, contrast and gamma to be altered. The gamma setting controlled the division of grey scale into the low, medium and high echo areas allowing certain areas to be more distinct. The Rejection Filter changed the range of the values of the received ultrasonic signals allowing the noise to be controlled.

Figure3.2 EchoBlaster User Interface used to obtain the best ultrasound image

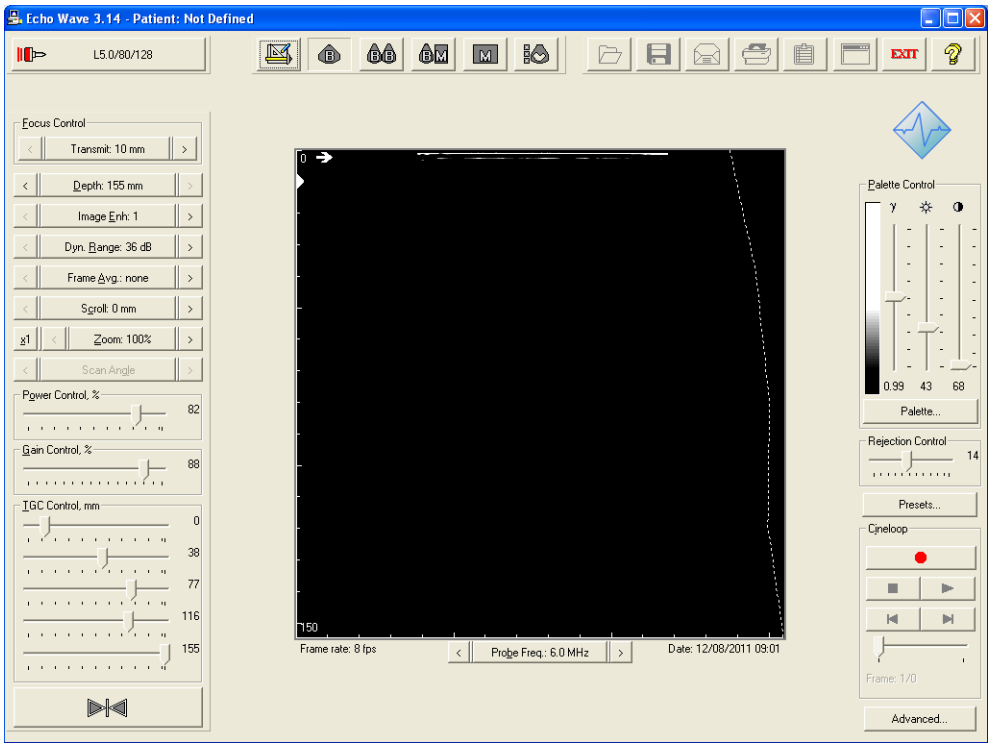

3.1.2 Navigation System

The navigation system also consisted of hardware and software which is detailed in the following subsections.

3.1.2.1 Hardware

The navigation system (OrthoPilot, B. Braun Aesculap, Tuttlingen, Germany) comprised of an optical tracking camera (Polaris, Northern Digital, Canada). The tracking system hardware consisted of two cameras (Fig 3.3) that emitted infrared light and registered the reflected light from the markers which had specific geometric arrangements of small spherical reflective markers allowing them to be individually identified (Fig 3.4). The reference point for the system consisted of one tracker marker. Attached to the ultrasound probe was a second marker.

Figure 3.3 & 3.4 Optical Tracking Camera, IR reflecting reference markers

3.1.2.2 Software

The software components used in the navigation system consisted of the OrthoPilot® user interface adjusted by B. Braun to incorporate the ultrasound images (Fig 3.5). In order to apply the settings for the ultrasound probe which provided the

optimal image in the EchoBlaster® software the files were edited. This was achieved by re-writing the XML files within the configuration settings directly. Microsoft Word was used to open the XML files and once the settings were found they were overwritten with the new settings. The settings of the OrthoPilot® system can be viewed in the appendix 1 in the appendices section. This allowed the ultrasound images to be related to marker coordinate data collected by the navigation system.

Figure 3.5 OrthiPilot® UI when performing a scan of the top of the femoral head

3.1.3 Combined Ultrasound & Navigation System

The combination of the ultrasound and navigation systems was facilitated by using the infrared cameras to locate specific marker sets within the field of view. Two marker sets were attached: one to the ultrasound probe and the other as the reference marker. The infrared camera independently located the two marker sets based on the individual geometric shape of the spherical reflective markers defining

each marker set. This enabled the OrthoPilot® software to attribute a point selected on the US image to a set of coordinates based on the point selected and the position of the ultrasound probe. The systems combine here by applying transformation algorithms between the different coordinate systems involved in the setup resulting in the point selected on the US image being converted into a set of coordinates relating its position to the external reference marker in the external reference marker coordinate system.

3.2 Validation (Blocks Testing)

3.2.1 Testing setup

The initial testing of the system involved an object of known geometrical properties (phantom) being scanned by the tracked ultrasound probe within a water bath. The water bath was selected based on the ease at which objects can be imaged when in a water bath compared to using other mediums for acoustic coupling. A digital calliper was used to measure the distances of each of the three dimensions of an acrylic block (60.1mm x 41.25mm x 14.75mm). This object of known dimensions was then fixed rigidly to the base of the water tank. The ultrasound probe with its tracker marker attached was positioned at the water/air interface with 1-2 cm of the linear probe submerged in the water. During data capture the probe was held in position using a series of clamps to ensure that the same image was recorded prior to the registration of each individual point. With the equipment correctly positioned an image was captured of one plane containing the point of interest. In order to obtain the coordinates of the exact location of interest a third tracker. Based on the geometric shape of the reflective marker the navigation system was able to use the third marker as a cursor to 'select' a location on the captured ultrasound image. This provided the coordinates of the point selected relative to the external marker in the external marker coordinate system. With the ultrasound image captured, the third tracker was used to select a location on the ultrasound image which represented the most proximal aspect of the object to the ultrasound probe. This was repeated on average between 10-15 times. The same process was performed selecting the aspect of the object on the ultrasound image which was most distal to the ultrasound probe. From this point it was possible to calculate the distance of the dimension of interest using the method detailed in the following subsection.

3.2.2 Method for calculation of distances

The method detailed in 3.2.1 provided two sets of 3-dimensional coordinates of the selected points of the same ultrasound image. As stated previously the coordinates were in the external marker coordinate system therefore in order to calculate the dimension being measured i.e. length, width or depth the 3-dimensional nature of these coordinates had to be taken into account. In order to ensure optimal results the points selected on the ultrasound image were lined up mainly with the Y direction of the ultrasound probe head. However as the ultrasound provided a two dimensional output there was the possibility of movement in the X and Z directions. Therefore in order to calculate the true distance between the two points the Cartesian version of Pythagoras's Theorem in 3 dimensional space between points (x_1, y_1, z_1) and (x_2, y_2, z_2) using equation 3.1 was applied where x_1 represented the x coordinate of the most proximal point, y_1 represented the y coordinate of the most proximal point and z_1 represented the z coordinate of the most proximal point. The second points represented the corresponding points but in relation to the distal point;

Equation 3.1 Calculation of distance between two points in Cartesian Coordinates

In order for this to be accurate, and avoid parallax error, the points selected on the image had to be directly above each other i.e. the distance measured was the perpendicular distance between the two surfaces (Fig 3.6).

Fig 3.6 Diagram depicting point selection on basic object

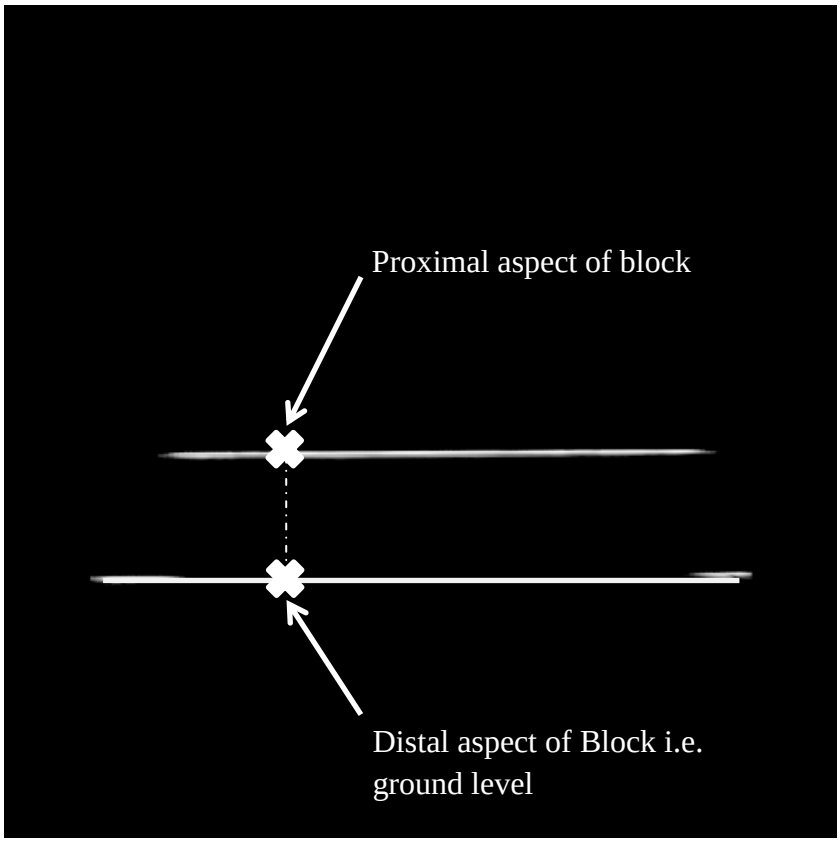

To improve the accuracy and precision of the plane based validation method a correction factor was applied to the results gathered as stated in chapter 2.3.2. Based on the temperature of the water of around 20° C the temperature correction factor was calculated as 0.96.

In terms of statistical analysis the data was subjected to basic descriptive statistics using analysis tool package within Microsoft Excel®. Using the statistical packages the results in terms of mean, standard deviation, standard error and confidence intervals were analysed.

3.3 Identification of Bony Landmarks

3.3.1 Design & Development of Bone Model

The accuracy and precision of the Ultrasound-based Navigation system was investigated further by applying the system to a solid foam femur model (Item no. #1120-20, Sawbones Europe AB, Krossverksgatan 3, 216 16 Malmö, Sweden, sawbones.com). The femur model was smaller than the average male femur length at 42 cm. It had a canal diameter of 15 mm, femoral head diameter of 45 mm and a lateral to medial condyle width of 69 mm.

The design of the base plate was developed collaboratively between myself, Angela Deakin (project supervisor) and Stephen Murray (departmental technician). The manufacturing aspect of the base plate was performed by Stephen Murray. The base for the sawbone was initially designed to allow the sawbone to be precisely positioned and fixed while the dimensions were being measured. This consisted of a base plate which slotted flush against the interior wall of the water tank. The base plate was constructed from an acrylic plastic of a sufficient density to stop the sawbone from floating. The acrylic plastic also provided the best possible surface for the ultrasound as it provided very little ultrasound image artefacts. The sawbone was placed roughly 85mm above the base plate by two acrylic pins and fixed to the pins by acrylic screws through the body of the femur (Fig 3.7).

Figure 3.7 Base Plate design with the femur sawbone attached

The body of the femur was selected as there were fewer anatomical points of interest at this section. The femur model was mounted on the base plate anterior side up with the proximal aspect of the model lying parallel with the base of the table. This provided the most level surface for the sawbone during construction resulting in a slight rotation of the distal aspect of the femur due to the structure of the bone. In the centre of the base plate steel screws were inserted to create a rectangular shape through the bottom surface to reveal 7mm of the screw protruding at the top of the plate. The edges of the screws were then filed down to create a well-defined point to allow easy detection for the ultrasound (Fig 3.8). These four points not only created the referencing points to which all the measurements on the femur were related to but also allowed the development of a reference coordinate system for the base plate coordinates.

Figure 3.8 Location of Reference Points on the Base Plate

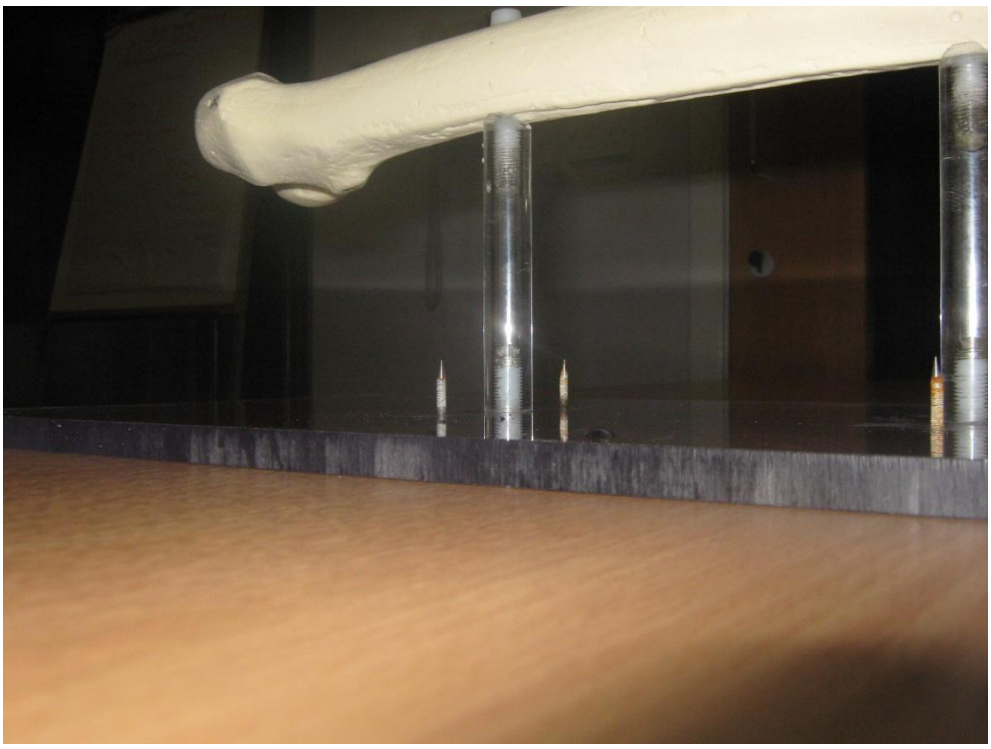

The anatomical landmarks of the femur selected for investigation included both proximal and distal aspects of the bone. These included proximally; the greater trochanter, lesser trochanter and femoral head diameter. Distal points of interest included; the medial epicondyle, lateral epicondyle, medial condyle, lateral condyle, adductor tubercle and the most posterior point on the lateral and medial condyles. Furthermore we decided to investigate the deepest point of the trochlear, the highest part of the intercondylar notch and the highest point of the anterior surface. These landmark locations were selected due to a variety of reasons including their importance in orthopaedic procedures as well as providing discussion points in terms of which landmark locations are more easily located than others. These points were marked on the femur with a marker pen so that they would not be visible on the ultrasound images resulting in the user being responsible for the location selection. The landmark locations were selected based on the Bartleby.com online version of Gray's Anatomy of the Human Body (www.bartleby.com/107/). The abbreviations used for the landmarks can be located in Table 3.1.

Landmark Location	Abbreviation
Greater Trochanter	GT
Lesser Trochanter	LT
Femoral Head Top	FHT
Femoral Head Bottom	FHB
Medial Epicondyle	ME
Lateral Epicondyle	LE
Medial Condyle	MC
Lateral Condyle	LC
Adductor Tubercle	AT
Intercondylar Notch	ICN
Femur Trochlear	FT
Anterior Aspect of Femur	ANT

Table 3.1 Abbreviations of Landmark Locations

3.3.2 ‘Gold Standard’ Measurement of Bone Model

The manual measurements were recorded of both the four reference points on the base plate and all the previously mentioned points of interest on the femur a total of five times each. This was performed by first defining the axis that we were going to use. The x axis was defined as the craniocaudal axis, the y axis was the mediolateral axis and the z axis was the anteroposterior axis. The spatial coordinates of each location were then selected using a Mitutoyo vernier height gauge which can measure distances of 0-600mm to within an accuracy of 0.02mm. The craniocaudalaxis (x) coordinates were found by measuring the vertical distance from the ground level to the point of interest with the base plate clamped 90° upright moving medially from left to right and proximally from the surface up (Fig 3.9). The mediolateral axis (y) coordinates were found by measuring the vertical distance from the ground level to the point of interest with the base plate clamped 90° upright moving distally from left to right and medially from the ground level upwards (Fig 3.11). The anteroposterior axis (z) coordinates were found by measuring the vertical distance from the ground level to the point location with the base plate flat on the surface moving distally from left to right (Fig.3.10). With the measurements recorded for each location in terms of their respective x, y and z heights gave each landmark location relative to the origin. From each landmark the mean was calculated giving ‘gold standard’ values of where all the landmark locations were.

Figure 3.9, 3.10 3.11 Base Plate Positions for measuring of x, y & z coordinates

3.3.3 Measurement of Bone Model with Ultrasound-based Navigation

The first stage of the ultrasound-based navigation system measurements involved locating the four reference points. This was achieved by placing the ultrasound probe with its tracker attached at the water/air interface with 1-2 cm of the linear probe submerged in the water. The ultrasound probe was then aligned as directly as possible with each reference point until a sharp point was clear on the ultrasound image. Similar to the methods adopted in the initial validation stage an image of the reference point was captured and then the location of the reference point was selected using the third tracker acting like a cursor. Each reference point was recorded a total of five times. This procedure provided the coordinates by which our base plate reference system could be defined.

The ultrasound-based navigation measurements were collected for each landmark location by placing the ultrasound probe with its tracker attached at the water/air interface with 1-2 cm of the linear probe submerged in the water (Fig 3.12)

Figure 3.12 US Probe positioned at Air/Water Interface

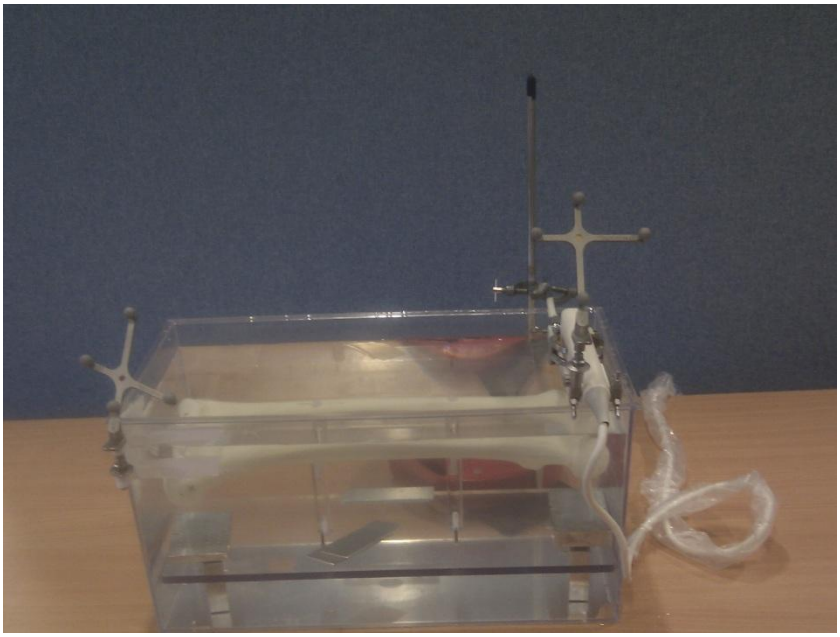

The probe was then aligned with the marked landmark location as accurately as visibly possible. With the landmark location visible on the ultrasound image the third tracker marker was used to select the landmark location based on the user's opinion. In order to introduce the repeatability of the test the ultrasound probe was removed from alignment and repositioned ensuring a new setup for each data collection. This process was repeated five times for each landmark location. Due to the combination of the anatomy of femur and the placement of the external reference marker at the top corner in order to capture some of the landmark locations the ultrasound probe had to be positioned on the outer wall of the tank (Fig 3.13).

Figure 3.13 US Probe positioned on side of water tank

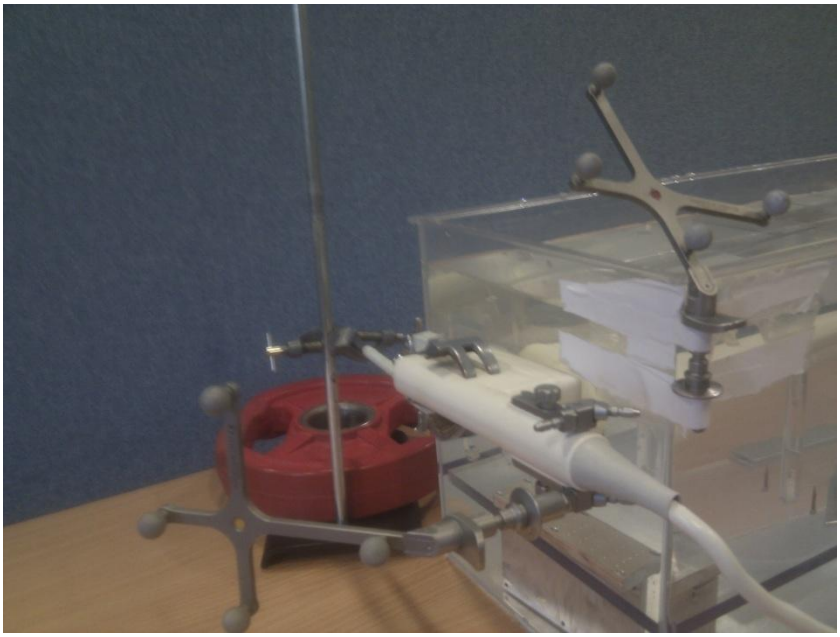

The acoustic coupling of the ultrasound probe to the tank wall was maintained using a conductive gel. Once the coordinates of all of the landmark location were found the data could be processed and converted into the required reference system.

3.3.4 Data Processing

3.3.4.1 Transformation of Ultrasound Coordinate System to Base Plate Coordinate System

To make the comparison between the Ultrasound-based Navigation data to the 'gold standard' landmark locations easier the ultrasound coordinate system was transformed to the base plate coordinate system. Transformations between any two coordinate systems have six degrees of freedom: three rotations (α, β, γ) and three translations(x, y, z).The rotation between the two coordinate systems is effected by rotating α around the x-axis, β around the y-axis, and γ around the z-axis and can be expressed as a general matrix, equation 3.2.

Equation 3.2 General rotation matrix

Using this convention equation 3.3 represents the calculation of the rotations between the two coordinate systems

Equation 3.3 Calculation of overall rotation matrix from three axis rotations

The rotation matrix [R] was calculated by first defining a common origin for which reference point four was selected. With this origin selected each of the other three reference points were calculated relative to this origin in both reference frames. Once the coordinates were from the same origin the rotation matrix could be

calculated. In order to calculate the rotational matrix we constructed unit vector matrices for each coordinate system as a result the different scales of each coordinate systems using equations 3.4 and 3.5.

Equation 3.4 Three coordinates in the external reference frame (erf)

Equation 3.5 Three coordinates in the base plate reference frame (bprf)

In equations 3.4 and 3.5, the subscript refers to one of three markers. With the coordinates of the three reference points in both reference systems known it was possible to calculate the rotation matrix based on equations 3.6a and 3.6b.

Equation 3.6a,b Calculation of Transformation Matrix

The coordinates in the base plate reference system essentially represents the product of the coordinates of the external reference system with the rotation matrix. The rotation matrix can therefore be calculated by rearranging the equation by multiplying the inverse of the external coordinates by the base plate coordinates. This process was not required for the initially block testing as the dimensions of the block could be found without the need to change coordinate systems.

In order for the rotation matrix to be accurate the two separate coordinates had to be in the same scale. This scale was calculated by from the magnitude of one

of the reference points (reference point three) in both reference frames. The scale factor was determined by dividing the magnitude of the coordinates of the external reference system by the magnitude of the coordinates of the base plate reference system. The external frame coordinates were then multiplied by this scale factor.

With this found the transformation matrix could be applied to the landmark locations to convert the external reference frame coordinates to base plate reference frame coordinates. The coordinates of the landmark locations were then multiplied with the rotation matrix to give the coordinates of the points selected in the base plate reference system.

This process allowed the direct comparison of the ultrasound-based navigation system to the manually measured values allowing the evaluation of the findings in terms of accuracy and precision.

3.3.4.2 Amendments to the Experimental Protocol

During the application of the transformation matrix to the landmark locations it came to the attention of me and my project supervisor, Dr Angela Deakin that the results were not as accurate as expected. This resulted in the experimental protocol being revised. Firstly the setup of the reference points was investigated. After deliberation it became apparent that as all the reference points were positioned at roughly the same height (z axis). Having all the reference points in the same z plane makes the mathematical procedures used in the rotation matrix very sensitive to small errors. From this it was hypothesised that errors in the ultrasound system, even for sharp points were large enough to put large errors into the rotation matrix. Secondly the directions of the axes of both coordinate systems were investigated and it was found that the x and y axis directions of the external reference system was in the opposite direction to the base plate reference system. The fact that these directions were opposite did not cause errors with the maths. However it made it harder to "see" the relationship between the numbers to check that they were roughly right. The rotation therefore helped visualise coordinates and check against the true values. After the revision of these two variables the procedure was performed again resulting in a new transformation matrix.

3.3.4.3 Analysis of Bone Landmark Accuracy & Precision

Once the values from both the manual measurement method and ultrasound method were in the same frame of reference the geometric values obtained from the 'gold standard' method could be compared to the results gathered from the ultrasound-based navigation system. This was done in a way similar to the calibration stage whereby all the coordinates of each landmark location in both measurement types can be related to the common origin.

In terms of statistical analysis the data was subjected to basic descriptive statistics using the statistics tool pack of Microsoft Excel®. The results obtained from testing were analysed in terms of mean, standard deviation, standard error and confidence intervals and compared to the 'gold standard' method.

4 Results

4.1 Validation of Hardware & Software

A total of 90 point location measurements were taken on a small acrylic block with dimensions 60.1mm x 41.3mm x 14.8mm. 30 measurements were taken of each of the 3 dimensions providing 15 calculated distances each for the length, width and depth of the block. Calibration means and descriptive statistical analysis of the planar dimensions are located in table 1 below.

Table 4.1 Comparison of Calliper measurements to values derived from the ultrasound and navigation systems

Dimension	Length	Width	Depth
Mean Caliper Measurement ± (mm)	60. 1± 0.02	41.3 ± 0.04	14.8 ± 0.02
Mean Ultrasound Measurement (mm)	60.4	41.4	14.8
Standard Error of US (mm)	0.05	0.11	0.09
Standard Deviation of US (mm)	0.21	0.42	0.35
True Difference (mm)	0.25	0.12	0.04
Percentage Difference (%)	0.42	0.3	0.27

Length. Length means and descriptive statistical analysis values are located in table 4.1. As an overall result, the 15 calculated distances for the length, with the temperature correction factor applied gave an average value of 60.4 mm. Testing on the length aspect of the block gave accuracy to within 0.25 ± 0.12 mm of the calliper measurements. The precision of the system can be inferred from the standard deviation (0.21 mm) and standard error (0.05) with maximum deviations of 0.61mm

positive and 0.08 mm negative. These values indicate that the systems accuracy and precision appear to be high due to these low values of mean, standard deviation and error.

Width. Width means and descriptive statistical analysis values are located in table 4.1. From the 15 calculated distances for width, with the temperature correction factor applied gave an average value of 41.37mm. Testing on the width aspect of the block gave accuracy to within 0.12 ± 0 of the calliper measurements. In terms of the precision of the measurements the low standard deviation and standard error values, 0.42mm and 0.11mm respectively combined with maximum deviations of 0.54 mm positive and 0.82 mm negative indicate that this navigation system combined with ultrasound provides precise measurements in this dimension.

Depth. Depth means and descriptive statistical analysis values are located in table 4.1. After applying the temperature correction factors to the depth values, from the 15 calculated distances for depth gave an average value of 14.79 mm. Testing on the depth aspect on the block gave accuracy to within 0.04 ± 0.19mm of the calliper measurements. In terms of the precision of the measurements the standard deviation and standard error values of 0.35 mm and 0.09 mm indicate that this navigation system combined with ultrasound provides relatively precise measurements measuring the length dimension. This is reinforced further by the maximum deviation values of 0.56 mm positive and 0.54 mm negative

4.2 Identification of Bony Landmarks

4.2.1 'Gold Standard' measurements

A total of 240 data points were collected on the revised base-plate with the attached femur sawbone. A sum of 60 of these data points provided the 4 reference point values with each reference point having its x, y and z value measured 5 times. The other 180 points provided the x, y and z coordinates of the 12 femur landmark locations with each location being measured 5 times. The mean values for these results are located in tables 2.1 and 2.2

Table 4.2 Mean Distance of Reference Points to selected origin (ref point 4)

Reference Point	Mean Distance from reference point 4 (mm)		
	x	y	z
1	139.92	0.62	0.21
2	139.77	66.50	52.78
3	-0.08	64.72	-0.04

Table 4.3 Mean Distance of selected Landmark Locations from Reference Point 4

Landmark Location	Mean distance from reference point 4 ± SD (mm)		
	x	y	z
GT	250.13 ± 0.1	9.91 ± 0.24	92.98 ± 0.14
LT	218.07 ± 0.18	45.88 ± 0.05	62.45 ± 0.26
FHT	277.91 ± 0.18	78.63 ± 0.08	110.38 ± 0.09
FHB	276.48 ± 0.14	84.76 ± 0.22	65.52 ± 0.2
ME	−126.55 ± 0.37	73.13 ± 0.25	61.57 ± 0.14
LE	−124.04 ± 1.28	− 0.6 ± 0.19	80.47 ± 0.11
MC	−156.83 ± 0.16	61.94 ± 0.22	58.83 ± 0.22
LC	− 153.18 ± 0.25	12.3 ± 0.12	72.49 ± 0.26
AT	−109.83 ± 0.16	53.36 ± 0.23	54.01 ± 0.12
ICN	−146.13 ± 0.29	35.49 ± 0.1	71.55 ± 0.15
FT	−137.5 ± 0.14	40.51 ± 0.2	91.22 ± 0.16
ANT	275.03 ± 0.35	81.66 ± 0.25	111.11 ± 0.06

4.2.2 Ultrasound & Navigation measurements

It was intended that a total of 240 data points were to be collected on the base-plate with the attached femur sawbone using the ultrasound and navigation system. A sum of 60 of these data points consisted of the 4 reference point values with each reference point having its x, y and z value measured 5 times. The other 180 points were to provide the x, y and z coordinates of the 12 femur landmark locations with the x, y and z value of each landmark being measured 5 times. Access to some of these locations using the ultrasound probe was restricted however resulting in not all landmarks being measured. The output from the ultrasound and navigation measurements were then subjected to the transformation procedure discussed in the methodology section providing us with the results of the ultrasound-based navigation system expressed in the base plate reference system. The proof of the calculation of the transformation matrix can be found in Appendix 2. The mean values for these results are located in tables 3.1 and 3.2.

Table 4.4 Scaled Mean Distances of Reference Points to selected origin (ref point 4)

Reference Point	Mean Distance from reference point 4 (mm)		
	x	y	z
1	137.80	6.34	0.12
2	142.24	-57.72	52.52
3	4.47	-63.6	1.56

Table 4.5 Mean Distance from Reference Point 4 (mm) with applied corrections

Landmark Location	Mean distance from reference point 4 (mm)		
	x	y	z
GT	251.39	7.73	97.27
LT	–	–	–
FHT	277.59	73.68	118.38
FHB	276.08	78.29	70.91
ME	-125.1	72.7	72.44
LE	–	–	–
MC	-162.51	60.99	64.76
LC	-158.07	12.05	81.51
AT	–	–	–
ICN depth	-148.46.	35.43	76.63
FT	-142.33	39.94	102.67
ANT height of FEM	274.12	77.27	118.74

4.3 Anatomical Accuracy & Precision

4.3.1 Accuracy

The accuracy of the ultrasound-based navigation system were analysed in terms of how similar the results of the US derived landmark locations were to the 'Gold Standard' measurements. These results have been tabulated in table 4.6 below.

Table 4.6 Distance between mean US-based and 'Gold Standard' measurements

Landmark Location	Distance of Mean from 'Gold' Standard value (mm)		
	x	y	z
GT	-1.26	3.64	-6.27
LT	–	–	–
FHT	0.32	4.95	-8.00
FHB	0.39	6.48	-5.39
ME	-1.44	0.43	-10.87
LE	–	–	–
MC	5.68	0.95	-5.92
LC	4.89	0.25	-9.02
AT	–	–	–
ICN depth	2.33	0.06	-5.07
FT	4.83	0.57	-11.44
ANT height of FEM	0.91	4.40	-7.63

X-axis. The accuracy of results of the x-axis values indicate the US-based navigation system could measure the x coordinate of the various landmark location to within a range of -1.44mm to 5.68mm. The most accurately definable landmark

locations in this axis were the Femoral Head Top (0.32mm) and the Femoral Head Bottom (0.39mm). The least accurate locations in this axis were the Medial Condyle and Lateral Condyle (5.68, 4.89 mm respectively).

Y-axis. The accuracy of results in terms of the y-axis values indicate the US-based navigation system could measure the y coordinate of the various landmark location to within a range of 0.25mm to 6.48mm. The landmark locations which provided the greatest accuracy in this direction were the Intercondylar Notch depth (0.06mm) and the Lateral Condyle (0.25mm). The least accurate landmark locations in this axis were the Femoral Head Top and the Femoral Head Bottom with values of 4.95mm and 6.48 respectively.

Z-axis. The accuracy of results in terms of the z-axis values indicate the US-based navigation system could measure the z coordinate of the various landmark location to within a range of -11.44 mm to -5.07mm. These results indicate that the system's ability to locate the coordinates of the z –axis was lower than its ability to accurately locate the x and y coordinates. The landmark locations which provided the greatest accuracy in this axis were the Intercondylar Notch depth (-5.07mm) and the Femoral Head Bottom (-5.39mm). The least accurate landmark locations in this axis were the Medial Epicondyle and the Trochlear of the Femur whereby the system was only able to measure the z coordinate to within -10.87mm and -11.44mm of their respective 'gold standard' values.

4.3.2 Precision

The precision (repeatability) of the ultrasound-based navigation system was analysed in terms of the variations in the results within each of the landmark locations. These results have been tabulated in terms of the standard deviations and standard errors for each landmark location and are located in Tables 4.7 and 4.8. The results can also be viewed graphically in the appendices section located at the end of the project. The standard deviation was selected as a statistically acceptable method of describing the precision of the US-based system as the standard deviation explains the variation of the data from the mean. A low standard deviation will indicate that the data will be close to the mean, whereas a high standard deviation will indicate that the data is more dispersed. Similarly the standard error was also selected as a statistically acceptable method of describing the system. The standard error of the mean provides the answer of how good our estimate of the mean actually is rather than how much variation exists around the mean. A high standard error value will indicate that there is a high amount of variation between the results used to calculate the mean value for each axis direction.

Table 4.7 Standard Deviations of Landmark Locations

Landmark Location	Standard Deviation, SD of US-based Landmark Locations (mm)		
	x	y	z
GT	1.01	0.93	0.74
LT	–	–	–
FHT	1.26	1.46	0.53
FHB	2.65	1.81	1.59
ME	0.66	0.47	0.80
LE	–	–	–
MC	0.11	0.74	0.52
LC	0.16	0.93	0.40
AT	–	–	–
ICN depth	0.39	0.54	0.15
FT	0.35	0.64	0.33
ANT height of FEM	1.20	1.28	0.35

X-axis. The results of the x axis coordinates show that the US-based navigation system gave a standard deviation ranging from 0.11mm for the Medial Condyle to 2.65 mm for the Femoral Head Bottom. In addition to the low SD for the Medial Condyle the Lateral Condyle (0.16mm) and Trochlear of the Femur (0.35mm) provided the lowest standard deviations indicating that these landmark locations had a high repeatability of landmark location. The higher standard deviations such as the Femoral Head Top (1.26mm) and Anterior Height of Femur (1.20mm) indicate the landmark locations which the system was less precise at finding.

Y-Axis. The results of the y axis coordinates show that the US-based navigation system gave a standard deviation ranging from 0.47mm for the Medial Epicondyle to 1.81mm for the Femoral Head Bottom. In addition to the low SD for the Medial Epicondyle the Trochlear of the Femur (0.64mm) and Intercondylar

Notch depth (0.54mm) provided the lowest standard deviations indicating that these landmarks could be found most precisely in the y coordinates The higher standard deviations of the Femoral Head Top (1.46mm) and Anterior Height of Femur (1.28mm) indicate the landmark locations which were found with less precision in terms of the y-axis value.

Z-axis. The results of the z axis coordinates show that the US-based navigation system gave a standard deviation ranging from 0.15mm for Intercondylar Notch to 1.59mm for the Femoral Head Bottom. In addition to the low SD for the ICN the Trochlear of the Femur (0.33mm) and Anterior Height of the Femur (0.35mm) provided the lowest standard deviations indicating that these landmarks could be found most precisely in the z-axis. The higher standard deviations of the Greater Trochanter (0.74mm) and Medial Epicondyle (0.8mm) indicate the landmark locations which were found with less precision with regards to the z-axis.

Table 4.8 Standard Error of Landmark Locations

Landmark Location	Standard Error, SE of the US-based Landmark Locations (mm)		
	x	y	z
GT	0.45	0.41	0.33
LT	–	–	–
FHT	0.56	0.65	0.24
FHB	1.18	0.81	0.71
ME	0.29	0.21	0.36
LE	–	–	–
MC	0.05	0.33	0.23
LC	0.07	0.42	0.18
AT	–	–	–
ICN depth	0.17	0.24	0.07
FT	0.16	0.29	0.15
ANT height of FEM	0.54	0.57	0.16

X-axis. The results of the x axis coordinates show that the US-based navigation system gave a standard error ranging from 0.05 mm for the Medial Condyle to 1.18 mm for the Femoral Head Bottom. In addition to the low SE for the Medial Condyle the Lateral Condyle (0.07mm) and the Trochlear of Femur (0.16mm) provided the lowest standard errors. These results indicate that these landmark locations had had the lowest variation between the repeated measurements. The higher standard errors such as the Femoral Head Top (0.56mm) and Anterior Height of Femur (0.54mm) indicate the landmark locations which had a larger degree of variation.

Y-Axis. The results of the y axis coordinates show that the US-based navigation system gave standard errors ranging from 0.21mm for the Medial Epicondyle to 0.81mm for the Femoral Head Bottom. In addition to the low SE for the Medial Epicondyle the Trochlear of the Femur (0.29mm) and Intercondylar Notch depth (0.24mm) provided the lowest standard error which again indicates a

lower variation between the measurements. The higher standard error values of the Femoral Head Top (0.65mm) and Anterior Height of Femur (0.57mm) indicating that these landmark locations had a greater degree of variation used to calculate the mean.

Z-axis. The results of the z axis coordinates show that the US-based navigation system gave a standard deviation ranging from 0.07mm for Intercondylar Notch to 0.71mm for the Femoral Head Bottom. In addition to the low SE for the ICN the Trochlear of the Femur (0.15mm) and Anterior Height of the Femur (0.16mm) provided the lowest standard errors. The results show that these landmark locations had the lowest variation indicating that the landmarks could be more precisely located in terms of their location in the z axis. The higher standard errors of the Greater Trochanter (0.33mm) and Medial Epicondyle (0.36mm) indicate the landmark locations which had a larger variation in the repeated measurements.

5 Discussion

5.1 Experimental Problems

Prior to the collection of data on the femur sawbone model there was a major problem regarding the ultrasound system. During the early validation stage of the project the ultrasound system began to malfunction resulting in the ultrasound image disappearing/reappearing intermittently. After review by the electronic technician within the bioengineering unit the apparatus was repaired and passed to be in suitable working order. This process rendered the apparatus out of working order for 3 days. After several weeks of use the system once again began to malfunction eventually resulting in its complete breakdown. After discussion it was decided that the ultrasound system was to be sent back to the company dealing with the product, BBraun (Lyon, France) to undergo testing and repair. Throughout this process the ultrasound system was unavailable for data collection for a total of two weeks. The result of this was that the testing and analysis on the second half of the project could not be completed as fully as intended due to the deadline for submission.

5.2 Comparison of Results to Previous Literature

5.2.1 Validation Stage of the Ultrasound-based Navigation System

The overall results from the initial validation stage indicate that the ultrasound-based navigation system was able to measure the various dimensions of the acrylic block to within a maximum distance of 0.25 mm, 0.12 mm and 0.04 mm for the length, width and depth respectively. It can be said that the validity of a measurement device irrespective of what it is measuring is its ability to provide a high level of accuracy and precision between the measured outputs to the true/real value. From these results it is evident that the system is sufficiently accurate when measuring basic geometric shapes when positioned in a specific orientation.

The accuracy at which the system including the tracker, IR camera and its software and the ultrasound system , including the probe and its software could possibly introduce a level of error. This has been shown by Schmerber and Chassatt (2001) who performed an in depth evaluation of the individual components of a navigation system. They concluded that the infrared camera was one of the main attributing factors to inaccuracies in measurements. The second potential source of error involves the resolution of the images recorded. For example if the ultrasound image has a low resolution there will be less pixels in the image meaning that the point selection stage will have fewer available points to select potentially introducing errors. The results from the initial validation stage of the investigation indicates that the accuracy of the ultrasound based navigation system was more than suitable based on the 0.5 to 3mm level of accuracy proposed by Khadem et al (2000). It can be concluded therefore that the accuracy demonstrated by the system provides a strong indication that the components of the system were functioning correctly and that there were no problems within the hardware or software of the system at the time.

The results achieved for this stage of the investigation can be reinforced by previously published literature. A similar study aimed at validating an ultrasound

system was performed by Riccabona et al (1996). In the study they investigated the distance measurements of a three dimensional ultrasound system. From the results they concluded a mean absolute error of 1.0 % (range, -2.3% to 1.9%) for the distances measured. These findings appear to reinforce the results obtained from the validation stage of the investigation where percentage error values of 0.41 % (range -0.13% to 1.02%), 0.29 % (range -0.82 to 0.54 % and 0.27 % (range -3.69% to 3.80%) were found for the length, width and depth respectively. Comparatively speaking however one disadvantage of the Riccabona study was that it did not incorporate any form of computer navigation system. Although the results appear to show similar findings a direct comparison cannot be made due to the different methodologies used.

Our results can however be compared to a more applicable methodology from a study performed by Lindseth et al (2003). In this study Lindseth investigated the navigation accuracy of an ultrasound-based navigation system whereby they compared automatically determined cross-wire phantom locations to physically measured locations. The accuracy of the system, which was represented by the mean distance between the two data selection types, was found to be 1.34 ± 0.62 mm. In comparison our results show similar findings indicating that our results are at an acceptable level of accuracy in terms of locating basic objects.

Our results are supported further when we compare them to one of the most accurate tests performed to date. Treece et al (2003) investigated a calibration of a 3D ultrasound system. In their testing they managed to reduce the level of error to 0.48mm at a depth of around 6cm. The validation test provided as accurate results to this at a similar scan depth. These findings help support the belief that the ultrasound-based navigation system provided acceptable results for objects of basic geometric shapes allowing the progression onto the next stage of the investigation.

Throughout the validation stage of this investigation the application of the correct speed of sound was essential in providing accurate results. The use of the wrong speed of sound would result in the misinterpretation of the geometry of the object within the volume area. As discussed previously the main difficulty with using ultrasound through the medium of water was that the speed of sound varies

significantly with temperature resulting in a slower speed than in the average soft tissue. As the experimental setup used water sourced from the tap which had a temperature of around 20°C. When the polynomial model for the speed of ultrasound in water initially proposed by Bilaniuk & Wong (1993) is applied to a water temperature of 20°C a speed of sound of 1482 m/s is calculated. As a result of this slower speed of sound in cold water the image obtained from the ultrasound probe would appear further away than its actual position. Studies have indicated that this variation in the speed of sound can give rise to valuation errors of around 5% for depth (Barratt et al, 2006). As described in the methodology section, the application of this correction factor translated the leading edge points towards the probe head effectively placing them closer to the true value. Without this correction factor the results in the initial validation stage would have been less accurate.

5.2.2 Femur Model

Looking at the overall results of the ultrasound-based navigation system on the femur model it can be concluded that although the system was unable to provide similar levels of accuracy to the current methods practised clinically, the system was sufficient at providing a relatively good level of accuracy considering the difficulties experienced throughout the project.

The results of the femur model show that there was a lower level of accuracy across the landmark locations in the z-axis compared to the x and y axis. Landmark locations such as the Medial Epicondyle and the Intercondylar Notch both provided the x and y axis locations to within 2mm of the true value. When the z axis value was investigated however there was a reduction in accuracy to over 5mm. Findings similar to these were found across the board for all the landmark locations with no landmarks being accurate to $\leq$ 5mm for the z axis and the worst being over 10mm out (Medial Epicondyle and Femoral Head Top). This could possibly be explained by the variations in the speed of sound through the medium of water. As described previously by Bilaniuk & Wong (1993) the slower the speed of sound in cold water is compared to the average soft tissue the further away the object will appear on the ultrasound image. Applying this theory to our project would theoretically determine z axis coordinates greater than there actual coordinates as no correction factors were applied to the femur model. Due to the complex nature of the femur model these correction factors could not be applied as the work developed by Bilaniuk & Woo was for basic single wall objects. Based on the results it is clear that the z coordinates were less accurate and the reason to why this was the case remains unclear. Barratt et al (2006) hypothesised that based on a simplistic model of how ultrasound propagates through various mediums the variations in the speed of sound could give rise to errors in locating the depth of the bone surface up to 5%. Research remains on-going in this area with the focus being around self-calibrating ultrasound probes.

From analysis of the femur model results it was evident that some landmark locations could be more accurately located than others using the ultrasound-based navigation system. The landmark locations such as the Medial Condyle and the

Intercondylar Notch provided the greatest overall accuracy to the 'gold standard' values when analysed graphically. From Appendix 5 for the Intercondylar Notch the graph depicting the x-y coordinates shows the extent of how accurate the data points are to the true coordinates. When the opposite end of the scale is investigated, for example the Lateral Condyle (Appendix 4) it is clear that although the y coordinate was fairly accurate the x and z coordinates were out by ≥ 4.89mm. The graphical representation of the Lateral Condyle clearly shows this where the low level of accuracy can be determined from the higher incidence of points indicating less accurate results.

As described previously the landmark locations of the Lesser Trochanter, Adductor Tubercle and the Lateral Epicondyle could not be found using the ultrasound probe due the problem of accessibility. The location of the Lesser Trochanter and Adductor Tubercle on the posterior aspect of the femur made it impossible for the ultrasound to penetrate through the sawbone and the probe could not be positioned in a way which provided a suitable image whilst maintaining line of sight with the Infrared camera. Whilst slightly disappointed that not all landmarks were accessible the results from the other landmark locations provide sufficient data for analysis.

In terms of the precision of the system the results on the femur model indicate that there is a relatively high repeatability of the ultrasound-based navigation system for the majority of the landmark locations. Low standard deviations and standard errors of landmark locations such as the Intercondylar Notch (Appendix 5) and the Lateral Condyle (Appendix 4) indicate that the ultrasound-based navigation system provided acceptable results in terms of repeatability. This is evident when they are compared graphically to less precise locations such as the Anterior Aspect of The Femur (Appendix 3) or the Femoral Head Bottom (Appendix 4). The tighter packed ultrasound points indicate a lower level of variation in the landmark selection. The graphs with fewer x and y points indicate a more accurate set of results which again supports the idea of greater precision. The standard deviation results for the majority of landmark locations of less than □1mm appear to be reinforced by Keppler et al (2004) who also investigated an ultrasound-based navigation system. In the study

they calculated an ultrasound-based system to have precision measurement of 1.17mm (SD). Taking this value as a marker for repeatability only two landmark locations produced higher standard deviations, the Femoral Head Top and Anterior Aspect of the Femur indicating that the ultrasound-based navigation system could provide suitable results in terms of precision.

Finally another potential source of error for the system involves the alignment of the scan plane with the landmark location. The difficulty with this aspect was that three dimensional coordinates are being generated from a selection of cross sectional images. If the ultrasound probe was not aligned correctly with the target landmark then it was possible that the wrong point on the landmark was being located introducing a level of error into the testing. This potential source of error can be directly linked to the accurate selection of the landmarks by the user. These findings are reinforced by Siston et al (2007) who concluded that the inaccurate location of landmarks by the user could lead to significant errors in the orientation within the coordinate system of use.

5.3 Application of Results to the Clinical Environment

Clinical studies incorporating various orthopaedic procedures have indicated that increased levels of accuracy are possible with navigated systems compared to traditional methods. Currently the primary method used in CAOS involves the attachment of a marker set directly to the bone at strategic locations around the joint and viewing the position with an infrared camera. This setup provides real-time spatial anatomical data regarding the position and orientation of the leg. However as described in section two one of the main disadvantages of this method is that it requires the fixation of the reference frame directly to the patient's anatomy throughout the operating procedure which gives rise to numerous disadvantages discussed previously.

Although non-invasive methods of fixation of the reference marker have been suggested as a potential area of further investigation there appears to be doubts regarding the level of inaccuracies due to the chances of excessive movement of the marker set. As the number of minimally invasive procedures continues to increase the interest for non-invasive methods of registration and data acquisition continues to grow as well.

The aim of this project was to investigate whether a non-invasive method of image capture by means of ultrasound could provide as accurate and precise results to the methods currently being employed. The results from our investigation indicate that there is still much to be considered with regards to the use of ultrasound as a method of navigation.

In terms of the application of the results to a clinical setting the investigation confirms that an ultrasound-based navigation system was unable to achieve as high a level of accuracy as the point-based registration methods currently being used. This is apparent when the results are compared to previous findings in the literature. Although the errors of some of the landmark locations fall within the range of 0.5 to 5 mm previously reported for navigation systems the level of error appears to be way off the 'gold standard' value of ~1mm

These findings are reinforced further by Lavalée et al (2004) who investigated a method of ultrasound-based registration on plastic bones encased in simulated soft tissue. From their study they reported a maximum error in measurement of 1.5mm. When we compare these findings to the results from the investigation it is evident that further research is required as overall landmark accuracy appears to be significantly greater than the values stated by Lavalée. If the x and y coordinates are investigated on their own however there appears to be evidence of some landmark locations approaching this level of accuracy. The Medial Epicondyle was located to within -1.43mm of its true value in its x axis and to within 0.43mm in its y axis indicating that the system was effective in in locating the landmark in this plane of view. Similar findings are evident for the Intercondylar Notch.

There does appear to be very little literature which has aimed at validating new techniques and procedures using clinically accurate ultrasound data. One study which has performed such a validation is by Amin et al (2003). They reported a mean RMS registration error of 1.27mm in translation for the pelvis of a patient using an ultrasound based system. They then compared the results to a commercially available technique known as the 'HipNav' protocol citing comparable results. More research involving clinical populations is required therefore in order to find out whether ultrasound-based navigation systems can be an effective alternative.

One previous study by Killian et al (2008) investigated the accuracy of a system known as *Echo Morphing* ® which combined free hand US image acquisition with a navigation system and applied it to fresh human cadavers. From the study they concluded that certain areas of the femur were more difficult to image than others. For example as a result of the position of the patella the femoral trochlear groove and distal condyles were more difficult to image. Furthermore the posterior intercondylar notch and femoral notch areas were also more difficult to visualize, as a result of the surrounding anatomy of the knee joint. The results from this study highlight the fact that when applied clinically the ultrasound technology comes up against further difficulties regarding accessing the bone surface from the surrounding anatomy.

Clinically it appears that the errors introduced from ultrasound-based registration methods would result in inaccurate location of landmarks on the bone surface. In procedures such as total knee arthroplasty the re-establishment of the alignment of the lower extremity to the mechanical axis is one of the fundamental goals (Sparmann et al, 2003). This procedure therefore requires the accurate location of the Femoral Head and Intercondylar Notch in order to realign the mechanical axis of the femur. From the results for these locations it can be concluded that the ultrasound-based methods investigated do not appear to provide as accurate results for these locations compared to the current methods used (Appendix 3 & 5). From this point of view the direct osseous registration remains the most accurate method for finding the mechanical axis.

The result from the ultrasound-based system on the femur model indicates that the landmark locations of the medial and lateral condyles could not be located as accurately as required. Clinically this finding proves significant for procedures such as total knee replacements. In these procedures the position of the Intercondylar Notch depth and the Femoral Trochlea creates the Whiteside line, which is used as a reference axis in total knee replacements. The accuracy at which these locations can be located will directly impact the alignment of the prosthesis which is essential for achieving the correct patellofemoral joint contact forces and correct rotational alignment of the tibia in extension (Middleton & Palmer, 2007) From the results it appears that the ultrasound-based navigation system cannot locate these landmarks to within a suitable level of accuracy indicating that the system cannot be used for this purpose.

The inaccuracies found in locating the depth of the bone in the investigation will significantly affect the efficacy of the ultrasound-based navigation systems use in the clinical environment. These levels of errors could be complicated further when applied to patients who are overweight or obese, potentially increasing the error in locating the bone surface up to several millimetres (Barratt et al, 2006). It is clear that the application of ultrasound-based systems warrants further investigation. Test protocols provide the perfect setting for gathering accurate and repeatable data. However, clinical populations will not provide these perfect settings. Patients who

are obese or have an abnormal anatomy will introduce difficulties for the system in locating the landmarks, introducing significant errors. These difficulties must be addressed before ultrasound-based navigation systems can be trialled with clinical populations.

From the investigation there appears to be several limitations which deserve further discussion. The implementation of the ultrasound-based navigation system into a clinical environment raises a number of key issues in terms of the ultrasound technology. As described previously there was the problem of accessing some of the landmark locations on the posterior aspect of the femur. The Lesser Trochanter, Adductor Tubercle could not be accessed by the ultrasound probe whilst maintaining the line of sight with the cameras. Furthermore the image quality was restricted by the operating frequency of the ultrasound probe. This highlights the requirement for all the components to be positioned perfectly to obtain results, a scenario which is not possible in the environment of the operating room.

The discussion points of access to landmark locations have also been discussed extensively in the literature. Data acquisition of a femur bone using ultrasound is relatively straightforward when investigating the femoral shaft as it has a basic shape with very few geometric features surrounded by muscle tissue. However this location is not really relevant for operative procedures such as THR and TKR. For example, one of the most surgically important areas of the anatomy of the femur during THR is around the femoral head and neck. Around this section the anatomy is far more complex. The higher incidence of tendons, ligaments as well as muscle tissue will result in the limited penetration depth of the ultrasound beam. Furthermore ultrasound imaging of the femoral head and neck is significantly obstructed by the acetabulum, preventing this region from being well-sampled. The difficulty of this task is increased further if the patient is overweight or obese where the penetration depth of the US probe may be inadequate. These limitations are consistent with a study by Barratt et al (2006) who reported that ultrasound imaging with limited access to the bone surface intraoperatively resulted in the introduction of depth-localisation errors due to the overlying soft tissue and lack of access to the bone.

6 Limitations of study

One limitation of this research project in terms of the relevance of the results in a clinical context was that the effects of underlying soft tissue were not taken into consideration. As the main focus of the project involved finding the accuracy and precision of the system the addition of a material which would mimic soft tissue was beyond the scope of the project. Results from previous studies investigating the combined accuracy of ultrasound and navigation systems have attempted to gather data for experimental setups aimed at replicating the conditions during CAOS surgery. One such method was proposed by Kilian et al. (2008) where they attempted to encase a femur bone with a foam coating to a similar thickness of the human thigh. The mimicking of the soft tissue affected the penetration depth and image quality of the ultrasound. They then developed the study further by performing the test on fresh cadaver specimens. By performing surface data acquisition using an ultrasound probe they were able to compare the results obtained to measurements taken from direct palpation of the bone surface after complete dissection of the cadaver. There results indicated that the system provided them with an accuracy of around 1mm which is sufficient for the majority of clinical applications. It is clear from these findings that the mimicking of soft tissue appears to be an obvious extension of this work.

Another limitation of this study was the use of a sawbone as the model of the femur. Due to the time frame of the project and the ethical pitfalls surrounding the use of human cadavers it was decided that a sawbone was the best alternative. Although sawbone models are manufactured to accurately resemble actual bone they are not adequate enough to fully replicate results from cadaveric specimens. As the sawbone was constructed from solid foam when positioned in the water tank the sawbone would float. This problem was resolved by sufficiently weighting the acrylic base plate to allow the sawbone to be fully immersed in the water. The use of a heavier plastic combined with a human cadaver would significantly improve the efficacy of the results.

The application of the system to the more clinically relevant object of the femur model further increased the potential sources of error through the calculation

of the transformation matrix. As discussed previously early testing with the 4 reference points of similar height z yielded a transformation matrix giving results nowhere near the expected values. After numerous amendments to the transformation procedure and reference point selection protocol discussed previously a working matrix was eventually generated. It was evident that the accurate selection of the reference points at the beginning of the data collection stage was vital for the correct calculation of the transformation matrix. It was evident that any minor errors in the locating of the reference points would propagate throughout the transformation matrix resulting in large errors in the transformed coordinates. This appears to be a limitation of the initial test protocol. With more registration points it would be possible to generate better algorithms for determining [R].

Finally the methodology used throughout the investigation had its limitations from a clinical point of view. The system allowed the landmark locations to be "seen" when aligned correctly with the probe. This would not be possible for actual clinical use however. In order to apply this system clinically a decision would have to be made on which plane would provide the best image. This comparison was not made and can be viewed as a limitation of the experimental protocol.

7 Conclusions

7.1 Conclusion

In conclusion, the use of an ultrasound-based navigation provided a non-invasive method of registering landmark locations to within a relatively suitable level of accuracy and precision. Although further research is required in order to remove the errors associated with the ultrasound technology it appears that ultrasound based imaging techniques could have a place in future methods. The ease at which ultrasound imaging can be performed whether it's pre-operative, intra-operative or post-operative makes it a viable alternative which could save health services millions of pounds. As ultrasound technology continues to improve the level of error discussed in this project should decrease. Through extensive research ultrasound-based navigation, in time could provide a safer, more accurate method of data acquisition for orthopaedic procedures.

7.2 Further Work

Both stages of the investigation involved the ultrasonic scanning through the medium of water. Future work could involve removing this probe/water interface and applying the navigation system to a femur model encased in a tissue mimicking material/ media similar to the study by Killian et al (2008). This could remove the potential errors from sound speed estimations and scaling issues for the 2D ultrasound image. The removal of the probe/water interface would remove the ambiguity of whether or not correction factor are required as well as providing a more clinically minded test setup.

Furthermore, clinically speaking the accuracy and precision of an ultrasound-based navigation system will be affected by the availability of the landmarks which the ultrasound probe can see. The results from this study indicate that certain femur landmark locations are easier to identify than others, a result which has been supported by previously reported studies. Therefore in order to fully test the true efficacy of an ultrasound-based navigation system further studies are required which incorporate a clinically relevant population as some landmark locations such as the intercondylar notch, which could be located relatively accurately in the investigation will not be visible when investigating a clinical population.

References

Amin DV, Kanade T, Di Gioia AM, 2001. Ultrasound based registration of the pelvic bone surface for surgical navigation. Computer Aided Surgery 6:48

Amiot AP and Poulin F, 2004. Computed tomography-based navigation for hip, knee, and spine surgery," Clinical Orthopaedics., vol. 421, pp. 77–86.

Amstutz C, 2003. A-mode ultrasound based registration in computer-aided surgery of the skull. Arch Otolaryngology Head Neck Surgery 129:1310–1316

Gray, Henry. *Anatomy of the Human Body.* Philadelphia: Lea & Febiger, 1918; Bartleby.com, 2000. www.bartleby.com/107/

Barratt, D.C., Penney, G.P., Chan, C.S., Slomczykowski, M., Carter, T.J., Edwards, P.J., Hawkes, D.J., 2006. Self-calibrating 3D-ultrasoundbased bone registration for minimally invasive orthopaedic surgery. IEEE Trans. Med. Imaging 25 (3), 312–323.

Bathis, H., Perlick, L., Tingart, M., Luring, C., Zurakowski, D., Grifka, J., 2004. Alignment in total knee arthroplasty. A comparison of computer assisted surgery with the conventional technique. Journal of Bone and Joint Surgery (British) Volume 86, 682–687.

Beckwith TH, Buck N, Marangoni R. Treatment of uncertainties mechanical measurements. 3rd ed. Boston

Bilaniuk N and Wong GSK. 1993. Speed of sound in pure water as a function of temperature. The Journal of the Acoustical Society of America, 93(3):1609{1612.

Brin YS, Livshetz IS, Antoniou JI, Greenberg-Dotan SI, Zukor1 DJ., 2010. Precise Landmarking in Computer Assisted Total Knee Arthroplasty Is Critical to Final Alignment. Journal of Orthopaedic Research 28:1355–1359

Chan CSK, Barratt DC, Edwards PJ, 1982. Cadaver validation of the use of ultrasound for 3D model instantiation of bony anatomy in image guided orthopaedic surgery. In Medical Image Computing and Computer-Assisted Intervention (MICCAI), 26–29 September 2004, Saint-Malo, France, Barillot C, Haynor DR, Hellier P (eds). Springer: Berlin, 2004; 397–404. n (MA): Addison- Wesley Publishing Company

Christensen, E.E., Curry,T.S., Dowdey, J.E.: Introduction to the Physics of Diagnostic Radiology: Lea & Febeger, Philadelphia, 2nd Ed. 1978. Chapter 25.

Delp SL, Stulberg SD, Davies B., 1998. Computer assisted knee replacement. Clinical Orthopaedic & Related Research 354:49– 56.

DiGioia III AM., 1998. What is computer assisted orthopaedic surgery? Journal of Clinical Orthopaedics. 354: 2-4

Fletcher J, Clark MD, Sutton FA, 1999. The cost of MRI: changes in costs 1989–1996. British Journal of Radiology. 72:432–437

Goss SA, Johnston RL, Dunn F., 1978 Comprehensive compilation of empirical ultrasonic properties of mammalian tissues. Journal of Acoustic Society of America 64:423-457.

Haaker, R.G., Stockheim, M., Kamp, M., Proff, G., Breitenfelder, J., Ottersbach, A., 2005. Computer-assisted navigation increases precision of component placement in total knee arthroplasty. Clinical Orthopaedics and Related Research, 152–159.

Heger S, Portheine F, Ohnsorge JA. 2005. User interactive registration of bone with A-mode ultrasound. IEEE Engineering in Medicine and Biology Magazine 24:85–95

Huang QH, Zheng YP, Lu MH, and Chi ZR. 2005. Development of a portable 3D ultrasound imaging system for musculoskeletal tissues. Ultrasonics, 43:153{163}

Hufner T, Geerling J, Kfuri M, Gansslen A(Jr), Citak M, Kirchhoff T, Sott TH, and Krettek C., 2003 “Computer assisted pelvic surgery: registration based on a modified external fixator,” Computer Aided Surgery, vol. 8, pp. 192–197

Hüfner T, Kendo V D, Citak M, Geerling J, Krettek C.,2006. Precision in orthopaedic computer navigation. Orthopaedics 35:1043–1055

IMV 2006 CT Market Summary Report. Des Plaines: IMV Medical Information Division.

Keppler P, Gebhard F, Grutzner PA, Wang G, Zheng G, Hufner T, Hankemeier S, Nolte LP., 2004. Computer aided high tibial open wedge osteotomy. Injury.35 Supplement 1: S-A68-78.

Khadem R, Yeh CC, Sadeghi-Tehrani M, Bax MR, Johnson JA, Welch JN, Wilkinson EP, Shahidi R., 2000. Comparative tracking error analysis of five different optical tracking systems. Journal of Computer Aided Surgery 5:98–107

Kowal J, Amstutz CA, Nolte LP., 2001 On B-mode ultrasound based registration for computer assisted orthopaedic surgery. CAOS/USA Meeting and Surgical Academy; Jul 6-8; Pittsburgh (PA)

Krysztoforski K, Krowicki P, Swiatek-Najwer E, Bedzinski R, Keppler P., 2011. Non-invasive ultrasonic measuring system for bone geometry examination. International Journal of Medical Robotics & Computer Assisted Surgery. 7: 85–95.

Lavallée S, Troccaz J, Sautot P, Mazier B, Cinquin P, Merloz P, and Chirossel JP., 1996. Computer-assisted spinal surgery using anatomy-based registration. Computer Integrated Surgery: Technology and Clinical Applications Eds. Cambridge, MA: MIT Press, pp. 425–446.

Lavallée S, Merloz P, Stindel E., 2004 Echo morphing: introducing an intra-operative imaging modality to reconstruct 3D bone surfaces for minimally invasive

surgery. In Langlotz F, Davies BL, Stulberg SD, editors. 4th Annual Meeting of CAOS International: June 16–19; Chicago, Illinois.

Li Q, Zamorano L, Jiang Z, Gong JX, Pandya A, Perez R, Diaz F., 1999. Effect of optical digitizer selection on the application accuracy of a surgical localization system - A quantitative comparison between the OPTOTRAK and flashpoint tracking systems. Journal of Computer Aided Surgery. 4:314–321

Lindseth. 2003 A robust and automatic method for evaluating accuracy in 3-D ultrasound-based navigation.

Lockwood GR, Turnbull DH, Christopher DA, and Foster FS. 1996. Beyond 30 MHz: Applications of high frequencies ultrasound imaging," IEEE Engineering in Medicine and Biology. vol. 15, no. 6, pp. 60-70.

Mason JB, Fehring TK, Estok R, Banel D, Fahrbach K., 2007 Meta-analysis of alignment outcomes in computer-assisted total knee arthroplasty surgery. Journal of Arthroplasty. 22:1097.

Matsuda S, Mizu-uchi H, Miura H, Nagamine R, Urabe K, Iwamoto Y. 2003. Tibial shaft axis does not always serve as a correct coronal landmark in total knee arthroplasty for varus knees. Journal of Arthroplasty.18 (1): 56-62.

Matziolis G, Krocker D, Weiss U, Tohtz S, Perka C (2007) A prospective, randomized study of computer-assisted and conventional total knee arthroplasty. Three-dimensional evaluation of implant alignment and rotation. Journal of Bone &Joint Surgery- American Version 89:236–243

McDicken . Diagnostic Ultrasonics. Principles and Use of Intruments

Middleton KR, Palmer SH., 2007. How accurate is Whiteside's line as a reference axis in total knee arthroplasty? Knee. Jun; 14(3):204

Mihalko WM, Krackow KA., 2006. Differences between extramedullary, intramedullary, and computer-aided surgery tibial alignment techniques for total knee arthroplasty. Journal of Knee Surgery; 19(1): 33-6.

Picard F, Laitner F, Gregori A, Martin P., 2007. A cadaveric study to assess the accuracy of computer-assisted surgery in locating the hip center during total knee arthroplasty. Journal of Arthroplasty. 22:590–5.

Murtha PE Watterson N, Nikou C, Jaramazi B., 2008 Accuracy of ultrasound to MR registration of the knee. International Journal of Medical Robotics& Computer Assisted Surgery. 4: 51–57.

Pitto RP, Graydon AJ, Bradley L, et al. 2006. Accuracy of a computer-assisted navigation system for total knee replacement. Journal of Bone Joint Surgery-British version. 88(5):601–605.

Prager RW, Rohling RN, Gee AH, and Berman L., 1998. Rapid calibration for 3-D freehand ultrasound. Ultrasound in Medicine & Biology, 24(6):855{869}.

Ritter MA, Faris PM, Keating EM, Meding JB. 1994. Postoperative alignment of total knee replacement. Its effect on survival. Clinical Orthopaedic Related Research. 299:153–6.

Sadowsky O, Yaniv Z, Joskowicz L. 2002. Comparative in vitro study of contact- and image-based rigid registration for computer-aided surgery. Computer Aided Surgery 7:223–236

Schmerber S, Chassat F. 2001. Accuracy evaluation of a CAS system: a laboratory protocol and results with 6D localizers, and clinical experiences in otorhinolaryngology. Computer Aided Surgery 6:1–13.

Simon DA.1996. Fast and Accurate Shape-based Registration. PhD Thesis, Carnegie Mellon University, Pittsburgh, PA.

Siston RA, Giori NJ, Goodman SB, Delp SL., 2007. Surgical navigation for total knee arthroplasty: a perspective. Journal of Biomechanics. 40:728–735.

Sparmann M, Wolke B, Czupalla H, Banzer D, Zink A., 2003. Positioning of total knee arthroplasty with and without navigation support. A prospective, randomised study. British Journal of Bone Joint Surgery. 85: 830-835.

Sprenger TR, Doerzbacher JF., 2003. Tibial osteotomy for the treatment of varus gonarthrosis. Survival and failure analysis to twenty-two years. American Journal of Bone Joint Surgery. 85:469-74.

Sugano N, Sasama T, Sato Y, Nakajima Y, Nishii T, Yonenobu K, Tamura S, and Ochi T., 2001. Accuracy evaluation of surface-based registration methods in a computer navigation system for hip surgery performed through a posterolateral approach," Computer Aided Surgery., vol. 6, pp. 195–203.

Treece GM, Gee AH, Prager RW,Cash CJC, and Berman LH. 2003. High-defnition freehand 3-D ultrasound. *Ultrasound in Medicine & Biology*, 29(4):529{546

.

Van Damme, G., Defoort, K., Ducoulombier, Y., Van Glabbeek, F., Bellemans, J., Victor, J., 2005. What should the surgeon aim for when performing computer-assisted total knee arthroplasty? Journal of Bone and Joint Surgery—American Volume 87 (Suppl 2), 52–58.

Vogt M, Opretzka J, Perrey C, Ermert H., 2010. Ultrasonic microscanning. Proceedings of the Institution of Mechanical Engineers Part H Journal of engineering in medicine. Volume: 224, Issue: 2, Pages: 225-240

Wells PNT., 1999. Ultrasonic imaging of the human body Reports on the. Progress in. Phyics. 62 671-722

Xu S, Shi Y and Kim SG., 2006. Fabrication and mechanical property of nano piezoelectric fibres. Journal of Nanotechnology 17 44-97.

Zheng, G., Ballester, M.A., Styner, M., and Nolte, L.P., 2006. Reconstruction of patient-specific 3D bone surface from 2D calibrated fluoroscopic images and point

distribution model. In: Proceedings of MICCAI (Pt 1), Lecture Notes in Computer Science, vol. 4190, pp. 25– 32.

Table of Appendices

XML Image Parameters

```
<?xml version="1.0" encoding="UTF-8"?>
-<ImageParam xmlns:NS0="http://www.w3.org/2001/XMLSchema-instance"
NS0:noNamespaceSchemaLocation="./ImageParam.xsd">
-<GroupUSG>
        <Name>L5/80/128</Name>
        <Main>
                <Size>14</Size>
                <Gain>2</Gain>
                <Power>95</Power>
                <DynRange>4</DynRange>
                <Beams>255</Beams>
                <Speed>1.540</Speed>
        </Main>
        <Freq>6MHZ</Freq>-
        <Agc>
                <Param>29</Param>
                <Param>143</Param>
                <Param>143</Param>
                <Param>143</Param>
                <Param>143</Param>
        </Agc>
        <Tfc>
                <Param>137</Param>
                <Param>64</Param>
                <Param>64</Param>
                <Param>64</Param>
                <Param>64</Param>
        </Tfc>-
        <Tgc>
                <Param>0</Param>
                <Param>35</Param>
                <Param>70</Param>
                <Param>105</Param>
                <Param>140</Param>
        </Tgc>
```

Appendix 1

```
-<Focus>
        <FocusSetNumber>2</FocusSetNumber>
        <FocusesInSet>4</FocusesInSet>

        -<FocusDepthAndGain>
                <DepthAndGain enabled="1" gain="229" depth="13"/>
                <DepthAndGain enabled="0" gain="212" depth="22"/>
                <DepthAndGain enabled="0" gain="200" depth="33"/>
                <DepthAndGain enabled="0" gain="195" depth="45"/>
        </FocusDepthAndGain>
</Focus>
-<AddFilters>
        <FrameAvg>0</FrameAvg>
        <SignalRejLowerBound>40</SignalRejLowerBound>
        <SignalRejUpperBound>255</SignalRejUpperBound>
        <SignalRejEnable>1</SignalRejEnable>
</AddFilters>
</GroupUSG>
-<Image>
        <Pos y="0" x="0"/>
        <Size y="768" x="1024"/>
        <Res y="7.36" x="7.36"/>
        <Org y="589" x="341"/>
        <Orient>0</Orient>
</Image>
-<Palette>
        <Gamma>1</Gamma>
        <Brightness>1</Brightness>
        <Contrast>50</Contrast>
        </Palette>
</ImageParam>
```

Appendix 1 cont.

Transformation Matrix Calculation

Taking the coordinates of the same four reference points in each coordinate system;

Base plate CS	taking reference point 4 as the origin		
	1	2	3
x	301.580	301.430	161.570
y	74.370	140.260	138.480
z	25.930	78.500	25.680

External CS	taking reference point 4 as the origin		
	1	2	3
x	296.558	301.000	163.225
y	173.201	109.139	103.254
z	-113.757	-61.350	-112.314

Coordinates are translated to Origin to give;

Translated to Origin		
1	2	3
139.924	139.774	-0.086
0.618	66.508	64.728
0.210	52.780	-0.040
	Sq. Root	64.728

1	2	3
137.799	142.240	4.466
6.341	-57.721	-63.606
0.118	52.526	1.562
	Sq. Root	63.782

Appendix 2

The External CS coordinates are then scaled and inverted to give;

Scaled Coordinates		
139.843	144.350	4.532
6.435	-58.578	-64.550
0.120	53.305	1.585

Inverse of External Coordinate System		
0.0072	0.0000	-0.0194
0.0000	0.0005	0.0194
0.0007	-0.0159	-0.0195

Rotation Matrix is then calculated by multiplying the inverse of the external coordinates by the base plate coordinates to give;

Final Rotation Matrix		
0.997	0.071	0.000
0.050	-0.999	0.014
-0.001	0.026	1.020

Landmark Locations in the base plate coordinate system can then be calculated by multiplying this matrix by the location in the External Coordinate System.

Appendix 2 continued

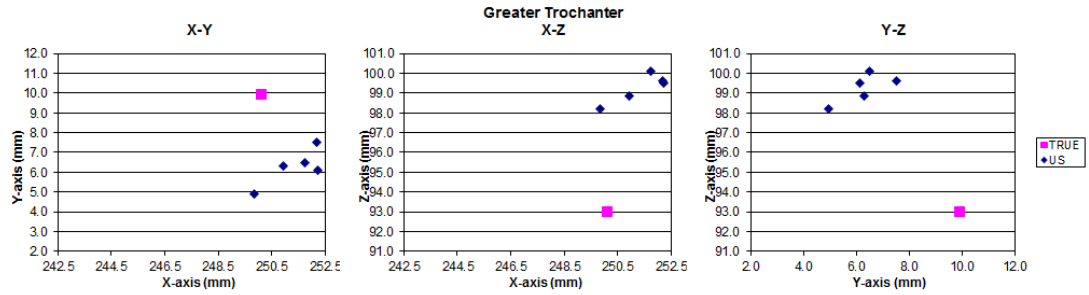
Greater Trochanter
X-Y
X-Z
Y-Z
Y-axis (mm)
Z-axis (mm)
X-axis (mm)
Y-axis (mm)
TRUE
US

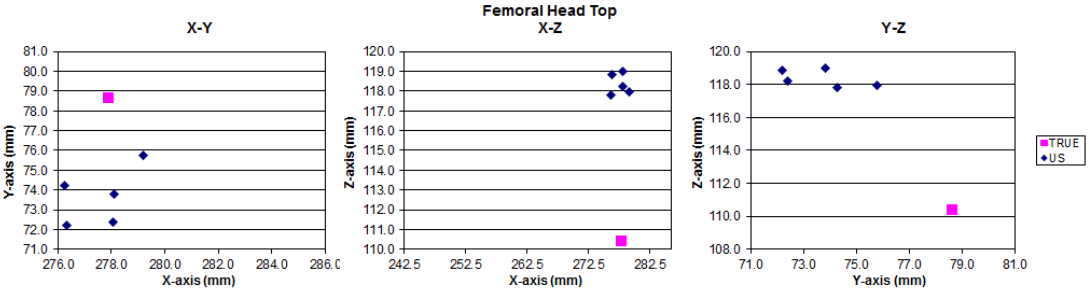
Femoral Head Top
X-Y
X-Z
Y-Z
Y-axis (mm)
Z-axis (mm)
X-axis (mm)
Y-axis (mm)
TRUE
US

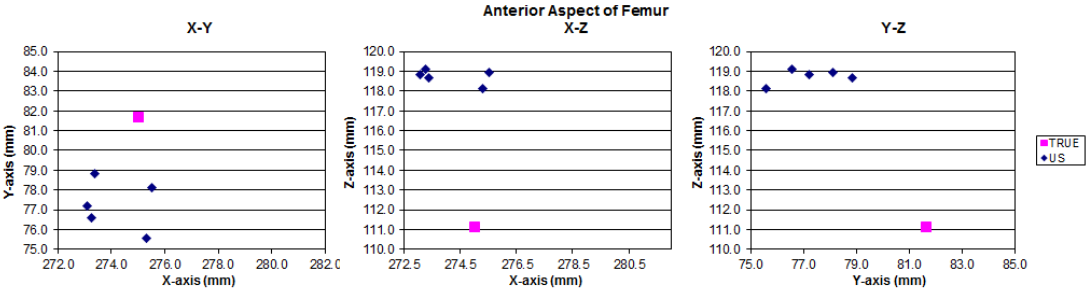
Anterior Aspect of Femur
X-Y
X-Z
Y-Z
Y-axis (mm)
Z-axis (mm)
X-axis (mm)
Y-axis (mm)
TRUE
US

Appendix 3

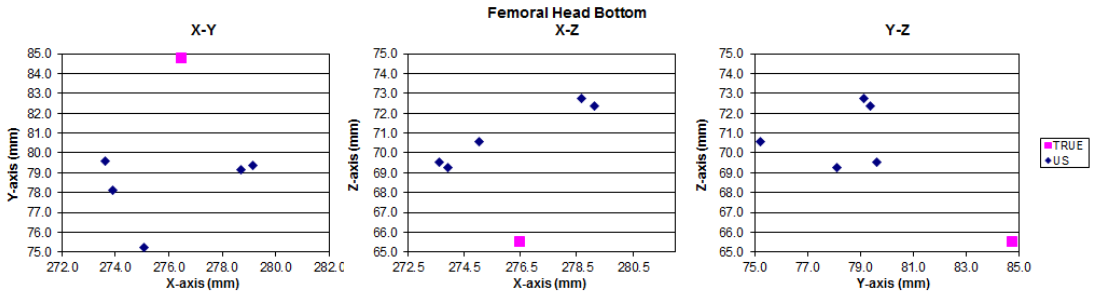
Femoral Head Bottom
X-Y
Y-axis (mm)
X-axis (mm)
X-Z
Z-axis (mm)
X-axis (mm)
Y-Z
Z-axis (mm)
Y-axis (mm)
TRUE
US

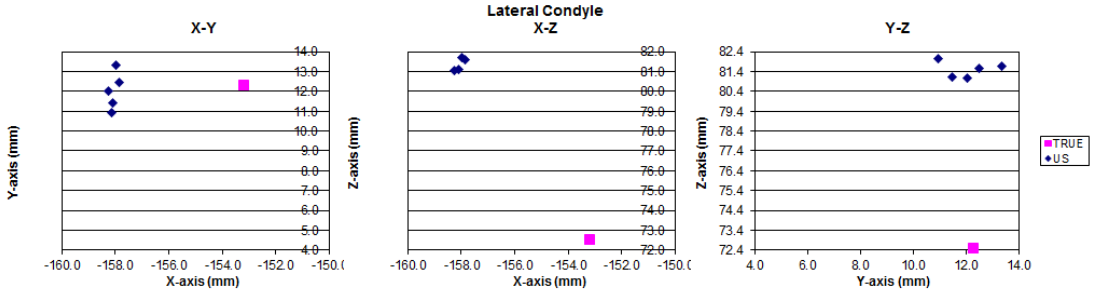
Lateral Condyle
X-Y
Y-axis (mm)
X-axis (mm)
X-Z
Z-axis (mm)
X-axis (mm)
Y-Z
Z-axis (mm)
Y-axis (mm)
TRUE
US

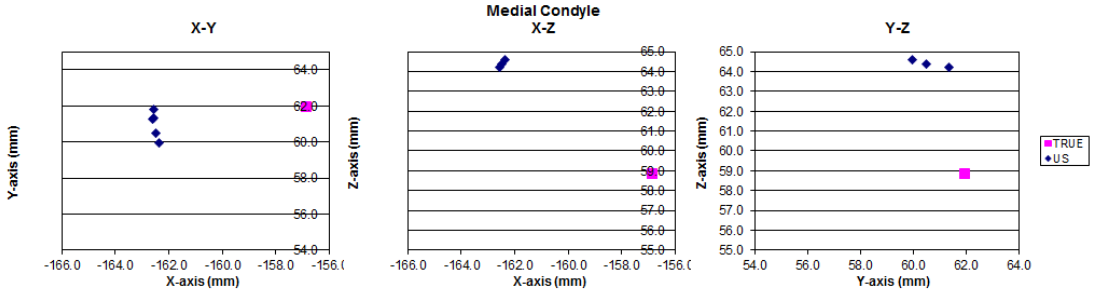
Medial Condyle
X-Y
Y-axis (mm)
X-axis (mm)
X-Z
Z-axis (mm)
X-axis (mm)
Y-Z
Z-axis (mm)
Y-axis (mm)
TRUE
US

Appendix 4

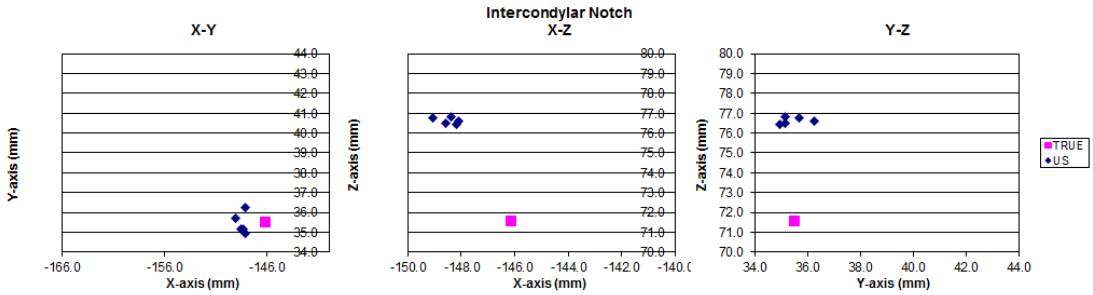
Intercondylar Notch
X-Y
X-Z
Y-Z
Y-axis (mm)
Z-axis (mm)
Z-axis (mm)
X-axis (mm)
X-axis (mm)
Y-axis (mm)
TRUE
US

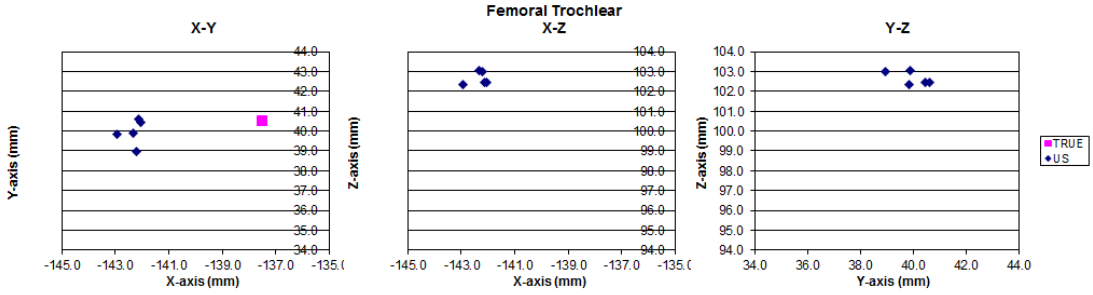
Femoral Trochlear
X-Y
X-Z
Y-Z
Y-axis (mm)
Z-axis (mm)
Z-axis (mm)
X-axis (mm)
X-axis (mm)
Y-axis (mm)
TRUE
US

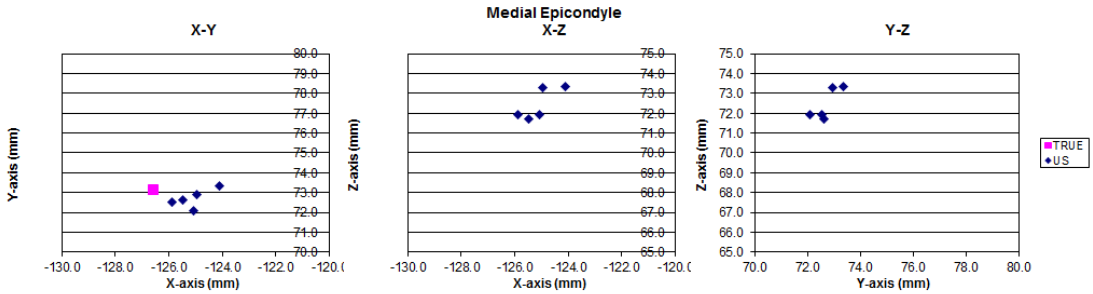
Medial Epicondyle
X-Y
X-Z
Y-Z
Y-axis (mm)
Z-axis (mm)
Z-axis (mm)
X-axis (mm)
X-axis (mm)
Y-axis (mm)
TRUE
US

Appendix 5